

Article

Single-Cell Transcriptome Atlas of Leaves at Different Developmental Stages in *Populus alba* × *Populus glandulosa* Clone 84K

Yanchun Jing¹, Yongyu Ren² , Shuwen Zhang¹ and Xiangyang Kang^{1,*}

¹ State Key Laboratory of Tree Genetics and Breeding, National Engineering Research Center of Tree Breeding and Ecological Restoration, College of Biological Sciences and Biotechnology, Beijing Forestry University, Beijing 100083, China; jingyanchun_81@163.com (Y.J.); shuwenzhang@bjfu.edu.cn (S.Z.)

² College of Forestry, Henan Agricultural University, Zhengzhou 450046, China; yongyuren_1128@163.com

* Correspondence: kangxy@bjfu.edu.cn

Abstract: Leaves are crucial photosynthetic plant organs. The development of poplar leaves has spatio-temporal specificity and it is of great significance to study the single-cell transcription atlas of leaves to reveal the temporal regulation of gene expression in different cell types. Here, single-cell RNA sequencing was performed on 17,768 tender leaf and 5846 functional leaf cells of Poplar 84K to construct a transcriptome atlas and developmental trajectory. The results showed that there were five and six cell types in tender and functional leaves, respectively. According to a pseudo-time trajectory analysis and the clustering of expressed genes into different cell types, the development of tender and functional leaves was divided into two temporal stages. Tender leaf epidermal cells developed earliest and were enriched with genes related to cell division and growth, indicating that tender leaves were in the stage of cell expansion and functional differentiation. Functional leaf palisade mesophyll cells were enriched with genes related to photosynthesis and carbon metabolism and cell types performing different functions tended to mature, indicating that functional leaves were in the stage of leaf development and the initial formation of photosynthesis. Our in-depth analysis of the transcriptional regulation at the single-cell level during leaf development provides an important basis for studying the mechanisms involved in cell differentiation and leaf development in poplar as well as other plants.

Keywords: leaf; cell types; single-cell RNA sequencing; temporal; transcriptome atlas



Citation: Jing, Y.; Ren, Y.; Zhang, S.; Kang, X. Single-Cell Transcriptome Atlas of Leaves at Different Developmental Stages in *Populus alba* × *Populus glandulosa* Clone 84K. *Forests* **2024**, *15*, 512. <https://doi.org/10.3390/f15030512>

Academic Editors: Evi Alizoti and Darius Kavaliauskas

Received: 14 January 2024

Revised: 7 March 2024

Accepted: 7 March 2024

Published: 9 March 2024



Copyright: © 2024 by the authors. Licensee MDPI, Basel, Switzerland. This article is an open access article distributed under the terms and conditions of the Creative Commons Attribution (CC BY) license (<https://creativecommons.org/licenses/by/4.0/>).

1. Introduction

Leaves are important tissues in plants, performing functions such as photosynthesis, transpiration, and gas exchange. Plants have evolved a wide variety of leaf shapes as a means of adapting to different environments. By increasing the chlorophyll density, plants maximize their ability to absorb sunlight, thereby providing fuel for the continuous production of the carbon substrates needed for vegetative and reproductive growth [1]. Moreover, leaf transpiration is the main driving force for the absorption of water and minerals by root systems [2,3].

The application of single-cell RNA sequencing (scRNA-seq) in plant research has become increasingly common [4–7]. Since the first high-resolution scRNA-seq expression atlas of Arabidopsis roots [8] was obtained, scRNA-seq expression atlases of leaves [6,9–14], roots [4,5,7,15–18], shoot apices [19], cotyledon veins [20], stomata [21], pigment glands [22], xylem [23–25], phloem [26], pollen [27,28], and female gametophytes [29], as well as other tissues and organs of Arabidopsis [6,11,16,19,20,29–31], rice (*Oryza sativa*) [13], bread wheat (*Triticum aestivum*) [17], corn (*Zea mays*) [32], tomato (*Solanum lycopersicum*) [33], rape (*Brassica rapa*) [10], chinese cabbage (*Brassica rapa*) [34], peanut (*Arachis subganea*) [3], cotton (*Gossypium bickii*) [22], crantz (*Manihot esculenta*) [14], poplar (*Populus*) [23–25,35], tea (*Camellia*

sinensis) [12], and bamboo (*Phyllostachys edulis*) [15] have been successively constructed. Based on the constructed single-cell transcriptome atlases of Arabidopsis, peanut, tea, and other plants, leaf cells can be divided into eight to twenty-six cell clusters assigned to seven to nine leaf cell types, including epidermal, mesophyll, vascular, proliferative, phloem, protoxylem, protophloem, palisade mesophyll, and procambium cells [3,6,10,12,13]. However, thus far, the single-cell transcriptome atlas of poplar leaves remains to be reported.

Poplar 84K (*Populus alba* × *P. glandulosa*) has had its entire genome sequenced [36] and tissue culture and genetic transformation are easily performed with this poplar hybrid. Accordingly, Poplar 84K has become a model plant material for forest molecular biology and genetic engineering research [37–39]. In this study, a single-cell transcriptome atlas of leaves at different development stages of Poplar 84K was constructed using scRNA-seq data. Subsequently, we classified the main cell types at each stage and identified the specific marker genes of the different cell types. We also evaluated the transcriptome differences among the leaves at the different developmental stages, described the developmental trajectories of cell types in tender and functional leaves, and inferred the gene expression characteristics that determine cell fates. According to the pseudo-time trajectory analysis and the clustering of expressed genes of different cell types, the development of tender and functional leaves was divided into two temporal stages. The results form a basis for the gene expression and functional analysis of poplar leaf development and provide valuable resources for future poplar molecular breeding research.

2. Materials and Methods

2.1. Protoplast Isolation of Leaves at Different Developmental Stages

Poplar 84K stem segments with terminal buds were transplanted to half-strength MS media [40], consisting of 0.02 mg·L⁻¹ 1-naphthaleneacetic acid (NAA) (Sigma, St. Louis, MO, USA), 0.05 mg·L⁻¹ indole butyric acid (IBA) (Sigma, USA), 3% (*w/v*) sucrose (Sigma, USA), and 0.6% (*w/v*) agar (Sigma, USA) (pH 5.8) for root formation. The tender (2nd leaf, N) and functional (5th leaf, fully expanded leaves, L) leaves [41,42] were removed from Poplar 84K sterile seedlings with a 40-day age. The fresh leaves were cut into 1–2 mm stripes. The tender leaf strips were immersed in an enzyme solution containing 2.0% (*w/v*) Cellulase RS (Yakult, Japan), 0.1%–0.2% (*w/v*) Macerozyme R-10 (Yakult, Japan), 0.1% (*w/v*) Pectolase Y-23 (Yakult, Japan), 3 mM 2-(N-morpholino) ethanesulfonic acid hydrate (MES) (Sigma, USA), 5 mM bovine serum albumin (BSA) (Sigma, USA), and 0.6 M D-mannitol (Sigma, USA) (pH 5.7). The functional leaf strips were immersed in an enzyme solution containing 2.5% (*w/v*) Cellulase RS, 0.5% (*w/v*) Macerozyme R-10, 0.2% (*w/v*) Pectolase Y-23, 3 mM MES, 5 mM BSA, and 0.6 M D-mannitol (pH 5.7). The leaf strips were then placed in a 27 °C incubator in darkness for 6 h. The cells were then filtered with a 40 µm cell strainer. Cell viability was detected by fluorescein diacetate (FDA) (Sigma, USA) staining and cell concentration was measured using a hemocytometer and light microscope (Figure 1d–g). Following this, protoplasts were resuspended in a 0.6 M mannitol solution in preparation for loading onto the chromium controller of the 10× Genomics platform (MGI Tech Co., Ltd., Wuhan, China). The concentration of protoplasts was adjusted to 1000 cells/µL for the construction of the scRNA-seq library.

2.2. Construction and Sequencing of the scRNA-seq Libraries

The scRNA-seq libraries were constructed with the Chromium Next GEM Single-Cell 3' Kit v.3.1 following the instructions of the user manual. The prepared protoplast suspension was loaded onto a 10× Genomics Chromium single-cell microfluidics device for the construction of the complementary DNA (cDNA) library. The DNA library was qualitatively analyzed using an Agilent 2100 Bioanalyzer (Waldbronn, Germany) and sequenced with a GISEQ-500 (MGI Tech Co., Ltd., Wuhan, China) sequencing platform.

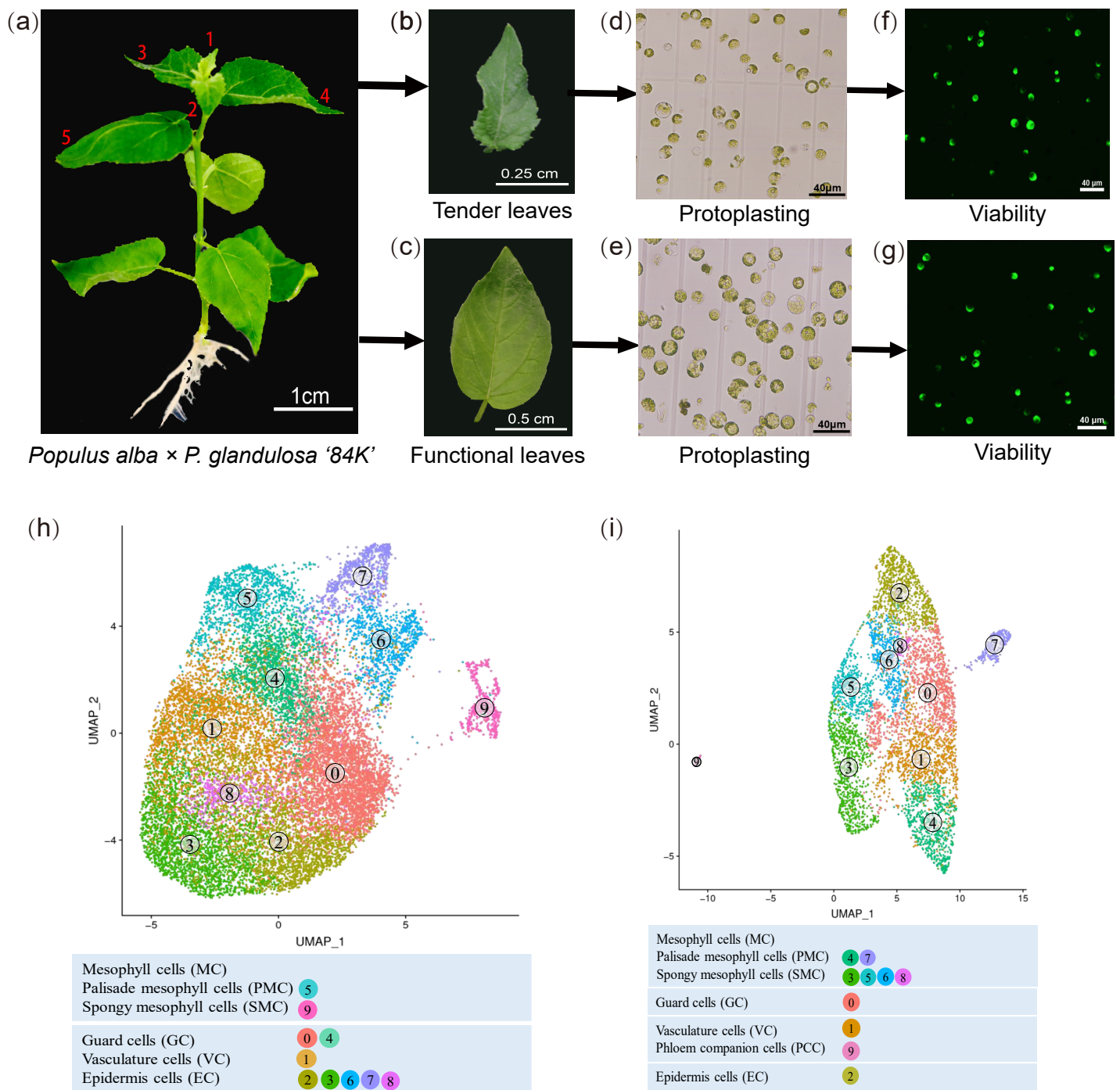


Figure 1. Protoplast isolation and construction of a single-cell transcriptome atlas of Poplar 84K leaves at different developmental stages. **(a)** Forty-day-old sterile seedlings; tender (2nd leaf) and functional (5th leaf) leaves are denoted as N and L, respectively. 1–5 represent different leaf positions. Scale bar = 1 cm. **(b)** Tender leaf. Scale bar = 0.5 cm. **(c)** Functional leaf. Scale bar = 0.5 cm. **(d,e)** Tender and functional leaf protoplasts were obtained by enzymatic hydrolysis. Scale bar = 20 μm. **(f,g)** Assessment of tender and functional leaf protoplast viability. **(h)** Classification of the distinct tender leaf cell clusters (UMAP atlas). Dots are individual cells ($n = 17,768$); colors distinguish the different cell clusters. **(i)** Classification of the distinct functional leaf cell clusters (UMAP atlas). Dots are individual cells ($n = 5846$); colors distinguish the different cell clusters.

2.3. Raw Data Quality Control

Cell Ranger (v.6.1.2) [43] was used to analyze the raw fastq data and generate the single-cell gene expression matrix. The Seurat R package (v.3.2.0) [44] was then used for downstream analysis. Cell quality control was carried out according to the number of detected genes and the proportion of mitochondrial reads (Figure S1). The doublets were identified and removed by DoubletDetection [45] and the cell cycle was analyzed with Seurat (CellCycleScoring function). After applying these quality control steps, 17,768 and 5846 single cells of tender and functional leaves remained and were included in the downstream analyses.

2.4. Data Visualization and Clustering

The gene expression data set was standardized and 2000 highly variable feature genes in the dataset were used for principal component analysis (PCA) [46]; a total of 50 principal components (PCs) were selected as input for a graph-based approach to cluster cells by cell type. The uniform manifold approximation and projection (UMAP) algorithm [47] was used for nonlinear dimensionality reduction analysis to simplify it for two-dimensional visualization and additional clustering. We used the Seurat function 'FindAllMarkers' to identify differentially expressed genes (cluster-enriched genes) for each cluster. The cluster-enriched genes were detected by parameters of "min. pct = 0.25" and "logfc. threshold = 0.25", which means the minimum cell percentage for differentially expressed genes (DEGs) is more than 0.25 and the \log_2 fold change of average expressions in more than 0.25. Then, the SCSA [48] method was used to annotate cell types. The differentially expressed genes in each cluster were associated with all possible cell types in the database to construct a 'cell-gene sparse matrix'. For each cell type in the matrix, SCSA scores each cell type through a decision model; the scoring results are related to the expression level of the marker gene and the prior association information between the marker gene and the cell type.

2.5. Marker Genes and Cell Type Identification

To identify the cell type, we first performed orthologous gene alignments of the reported marker genes in Arabidopsis. The marker gene list was downloaded from the Plant Cell Marker DataBase (PCMDB, <http://www.tobacodb.org/pcmdb/>) [12,49]. In this study, gene ontology (GO) and Kyoto Encyclopedia of Genes and Genomes (KEGG) enrichment analyses were performed on the identified differential genes. The differentially expressed genes of TOP10 in cell clusters were selected and KEGG and GO enrichment annotations were performed to construct enrichment heat maps (Figures S6–S9) for different cell types (Tables S3 and S4). Following this, we selected cluster-specific marker genes and assigned all clusters to specific cell types.

2.6. Pseudo-Time Trajectory Analysis

Single-cell trajectories at different developmental stages were constructed using Monocle (v.2.0) [50]. First, the "diffvGeneTest" function was used to calculate the differentially expressed genes in different regions. The "dispersion table" function was used to select highly variable feature genes. The overlapping genes between differentially expressed genes and highly variable feature genes in different regions were used for the subsequent analysis. Following this, we employed the reverse embedding (DDRTree) algorithm to reduce the data dimensions while Monocle ordered the cells. Then, we ordered the cells using the orderCells function. Once the cells were ordered, we visualized the trajectory using plot_cell_trajectory in the reduced dimensional space. In addition, we needed to call orderCells again with the root_state parameter to specify the beginning. Monocle used the Branch Expression Analysis Modeling (BEAM) method to analyze the cell data after pseudo-time and the designated nodes to mine the DEGs related to the branches and used the plot_genes_branched_heatmap function to draw the expression heat map of the genes

at different branch points or states. The `num_clusters` parameter in this function clustered the data. Heatmaps were used to demonstrate the gene expression that differs in cells.

3. Results

3.1. Leaf Cell Type Identification at Different Developmental Stages

To explore the cell heterogeneity of leaves at different developmental stages of Poplar 84K, we isolated protoplasts from tender (second leaf) (Figure 1a,b) and functional (fifth leaf) leaves (Figure 1a,c) of 40-day-old sterile seedlings. The protoplasts (17,768 tender and 5846 functional leaf cells) (Figure 1d–g) were then loaded into the 10X Chromium platform for scRNA-seq analysis to generate the single-cell transcriptome atlas. Additionally, cDNA libraries were then generated and sequenced and the data were filtered at both the cell and gene levels. Approximately 54,221 reads and a median of 2124 genes were detected per tender leaf cell and 146,263 reads and a median of 1262 genes were detected per functional leaf cell for further analysis (Table S1).

Each cell cluster of Poplar 84K leaves was annotated according to the expression of homologous genes in the published scRNA-seq data for Arabidopsis (Table S2). In addition, cell marker genes were identified for each cluster detected in the leaves of Poplar 84K (Tables S3 and S4). GO and KEGG pathway analyses were performed on all cell populations to reveal the potential biological functions of genes expressed in each cell cluster to evaluate the method used in identifying specifically expressed cell-type genes and the ability to correctly attribute biological processes to a cell type (Figures S2–S9 and Tables S3–S8). Based on these information sources, Poplar 84K tissue-specific marker genes were selected for the annotation of the main cell clusters. The results showed that the tender leaves were grouped into ten distinct cell clusters, which were assigned to five cell populations—epidermal cells (ECs; Clusters 2, 3, 6, 7, and 8), guard cells (GCs; Clusters 0 and 4), palisade mesophyll cells (PMCs; Cluster 5), sponge mesophyll cells (SMCs; Cluster 9), and vascular cells (VCs; Cluster 1) (Figure 1h). The functional leaves were also grouped into ten distinct cell clusters, which were assigned to the following six cell populations: ECs (Cluster 2), GCs (Cluster 0), PMCs (Clusters 4 and 7), SMCs (Clusters 3, 5, 6, and 8), VCs (Cluster 1), and phloem companion cells (PCCs) (Cluster 9) (Figure 1i).

3.2. Gene Expression Characteristics of Epidermal Cells in Tender and Functional Leaves

The ECs of tender leaves were composed of Clusters 2, 3, 6, 7, and 8, in which 1329 DEGs were expressed. Clusters 2 and 3 were mainly enriched with genes related to fatty acid biosynthesis and metabolism, stress resistance, and respiratory metabolism. The genes associated with fatty acid biosynthesis were *CHLOROPLASTIC ALDO-KETO REDUCTASE (ChIAKR)*, *12-OXOPHYTODIENOATE REDUCTASE 2 (OPR2)*, and *LIPID PHOSPHATE PHOSPHATASE 3 (LPP3)*; the genes related to stress resistance were *LUMINAL BINDING PROTEIN 2 (BIP2)* and *GLUTATHIONE TRANSFERASE L3 (GSTL3)*; and the genes related to respiratory metabolic were *ACONITASE 1 (ACO1)* and *ACO3*. The genes in Clusters 6, 7, and 8 were mainly associated with fatty acid biosynthesis and metabolism, stress resistance, plant hormone signal transduction, and cell growth function. The top five genes related to fatty acid biosynthesis were *LIPID TRANSFER PROTEIN 1 (LTP1)*, *Li-TOLERANT LIPASE 1 (LTL1)*, *3-KETOACYL-COA SYNTHASE 10 (KCS10)*, *KCS11*, and *ECERIFERUM 1 (CER1)*; the genes linked to stress resistance were *PATHOGENESIS-RELATED 3 (PR3)* and *POM-POM1 (POM1)*; and the genes related to plant hormones were *SOLITARY ROOT (SLR)*, *INDOLE-3-ACETIC ACID INDUCIBLE 4 (IAA4)*, and *IAA17*. The genes most associated with cell growth function were *EXPANSIN L2 (EXPL2)*, *EXPA8*, and *XYLOGLUCAN ENDOTRANSGLUCOSYLASE/HYDROLALASE 16 (XTH16)*. Functional leaf ECs comprised Cluster 2, in which 759 DEGs were expressed. Cluster 2 was mainly enriched with genes related to unsaturated fatty acid and fatty acid biosynthesis and metabolism, respiratory metabolism, and stress resistance. The genes associated with unsaturated fatty acid and fatty acid biosynthesis and metabolism were *OPR2* and *FATTY ACID DESATURASE 2 (FAD2)*; the genes related to respiratory metabolism were *ACO3* and

GLUCOSE-6-PHOSPHATE DEHYDROGENASE 6 (*G6PD6*); and, finally, the genes linked to stress resistance were *ETHYLENE RESPONSE FACTOR 1 (ERF1)* and *BIP2* (Figure 2a–c and Tables S3 and S4).

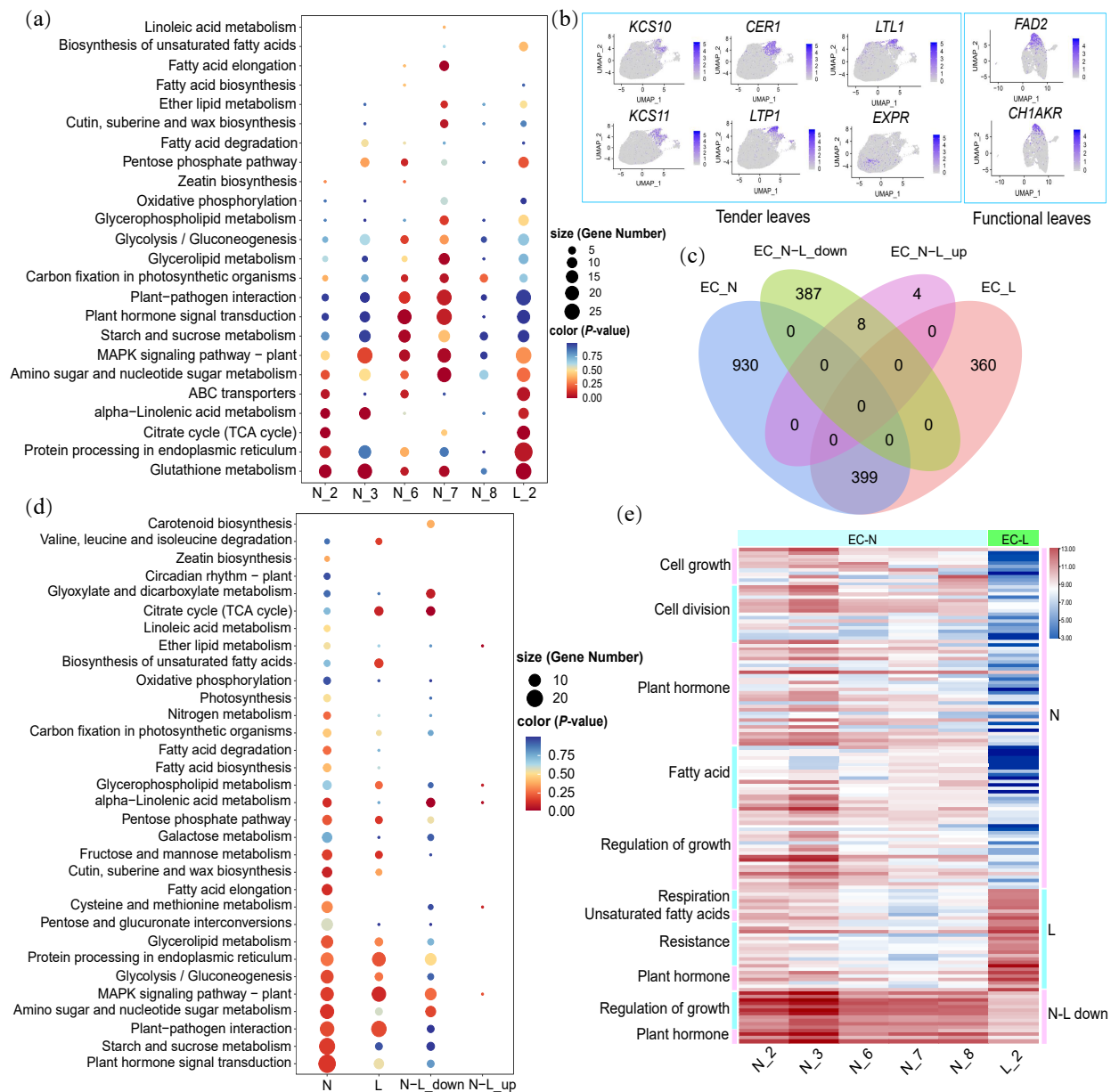


Figure 2. Differentially expressed genes (DEGs) analysis of epidermal cells (ECs) of leaves at different developmental stages. **(a)** Kyoto Encyclopedia of Genes and Genomes (KEGG) functional enrichment of genes in different cell clusters of tender and functional leaves. Color (*p*-value) represents the degree of pathway enrichment; details are given in Table S10. **(b)** The main marker genes in ECs of leaves at different developmental stages. **(c)** A Venn diagram showing the number of genes expressed during the two stages of leaf development. **(d)** KEGG functional enrichment analysis of four gene clusters at two leaf developmental stages. Color (*p*-value) represents the degree of pathway enrichment; details are given in Table S11. N: genes expressed only in tender leaves; L: genes expressed only in functional leaves; N-L_down (up): down-regulated and up-regulated genes in co-expressed genes. **(e)** Heatmap of functional analysis of DEGs expressed separately with different expression trends in ECs of tender and functional leaves. The color bar indicates the relative expression level (red = high, blue = low).

Venn diagram analysis showed that 399 DEGs were co-expressed in ECs while 930 and 360 DEGs were specifically expressed in tender and functional leaves, respectively

(Figure 2c and Table S9). Genes involved in fatty acid elongation; cutin, suberine, and wax biosynthesis; plant–pathogen interactions; and glycolysis/gluconeogenesis were significantly expressed in the tender-leaf stage. Genes with roles in the biosynthesis of unsaturated fatty acids, the citrate cycle (TCA cycle), and plant–pathogen interactions were significantly expressed mainly at the functional-leaf stage. Among the genes that were highly expressed at both developmental stages, the expression levels of those associated with the biosynthesis of unsaturated fatty acids and the respiration pathways gradually increased with continued leaf development. The expression of genes related to fatty acid elongation, fatty acid biosynthesis, alpha-linolenic acid metabolism, glycerolipid metabolism, and cell growth function exhibited the opposite trend (Figure 2d,e and Tables S10 and S11).

3.3. Gene Expression Characteristics of Guard Cells in Tender and Functional Leaves

The GCs of tender leaves comprised Clusters 0 and 4, in which 491 DEGs were expressed. Cluster 0 was mainly enriched with genes related to photosynthesis, fatty acid biosynthesis and metabolism, and respiratory metabolism. The genes with roles in photosynthesis were PHOTOSYSTEM II REACTION CENTER PROTEIN C (PSBC) and *YCF2.1*; the genes associated with fatty acid biosynthesis and metabolism were *LIPOXYGENASE 3 (LOX3)* and *AOC3*; and the respiratory metabolism-related genes were *H(+)-ATPASE 5 (HA5)* and *ATP SYNTHASE ACCESSORY FACTOR ATPL (ATPI)*. Cluster 4 was mainly enriched with genes related to fatty acid biosynthesis and metabolism and stress resistance. The genes involved in fatty acid biosynthesis were *LOX3*, *DELAYED DEHISCENCE 2 (DDE2)*, and *KCS11* while the genes related to stress resistance were *CALMODULIN-LIKE 11 (CML11)* and *Ca²⁺-BINDING PROTEIN 1 (CP1)*. The GCs of functional leaves were composed of Cluster 0, in which 612 DEGs were expressed. Cluster 0 was primarily enriched with genes with stomatal-specific expression and genes related to unsaturated fatty acid and fatty acid biosynthesis and metabolism, respiratory metabolism, starch and sucrose metabolism, and photosynthesis. The stomatal-specific gene was *MIGOGEN-ACTIVATED PROTEIN KINASE 3 (MPK3)*. The genes associated with unsaturated fatty acid and fatty acid biosynthesis and metabolism were *OPR2*, *FAD2*, and *KCS11*; the genes related to respiratory metabolism were *ACO3* and *HA5*; the genes associated with starch and sucrose metabolism were *SUCROSE SYNTHASE 3 (SUS3)* and *CELL WALL INVERTASE 2 (CWINV2)*; and the genes with roles in photosynthesis were *PHOTOSYSTEM I SUBUNIT D-2 (PSAD-2)* and *PHOTOSYSTEM I REACTION CENTER SUBUNIT PSI-N (PSAN)* (Figure 3a–c and Tables S3 and S4).

Venn diagram analysis showed that 140 DEGs were co-expressed in GCs while 351 and 472 DEGs were specifically expressed in tender and functional leaves, respectively (Figure 3c and Table S12). Genes involved in plant–pathogen interactions, photosynthesis, and alpha-linolenic acid metabolism showed significant expression in the tender-leaf stage. Meanwhile, genes involved in glycolysis/gluconeogenesis, starch and sucrose metabolism, were significantly expressed in the functional-leaf phase. Among the genes that were significantly expressed at the two development stages, those associated with photosynthesis, fatty acid biosynthesis and metabolism-related pathways, and starch and sucrose metabolism showed a trend of increasing expression with continued leaf development. However, genes involved in alpha-linolenic acid metabolism and plant–pathogen interaction pathways showed the opposite trend (Figure 3d,e and Tables S13 and S14).

3.4. Gene Expression Characteristics of Palisade Mesophyll Cells in Tender and Functional Leaves

The PMCs of tender leaves consisted of Cluster 5, in which 532 DEGs were expressed. Cluster 5 was mainly enriched with genes associated with photosynthesis and carbon fixation in photosynthetic organisms. The major genes involved in photosynthesis were *LIGHT-HARVESTING CHLOROPHYLL-PROTEIN COMPLEX II SUBUNIT B1 (LHCB1.4)*, *RIBULOSE BIPHOSPHATE CARBOXYLASE SMALL CHAIN 1A (RBCS1A)*, and *PHOTOSYSTEM I SUBUNIT H2 (PSI-H)*. The PMCs of functional leaves comprised Clusters 4 and 7, in which 654 DEGs were expressed. Clusters 4 and 7 were mainly enriched with genes

related to photosynthesis and carbon fixation in photosynthetic organisms. The major genes associated with photosynthesis were *LHCB1.4*, *PHOTOSYSTEM II SUBUNIT R (PSBR)*, and *RBCS1A* (Figure 4a–c and Table S3 and S4).

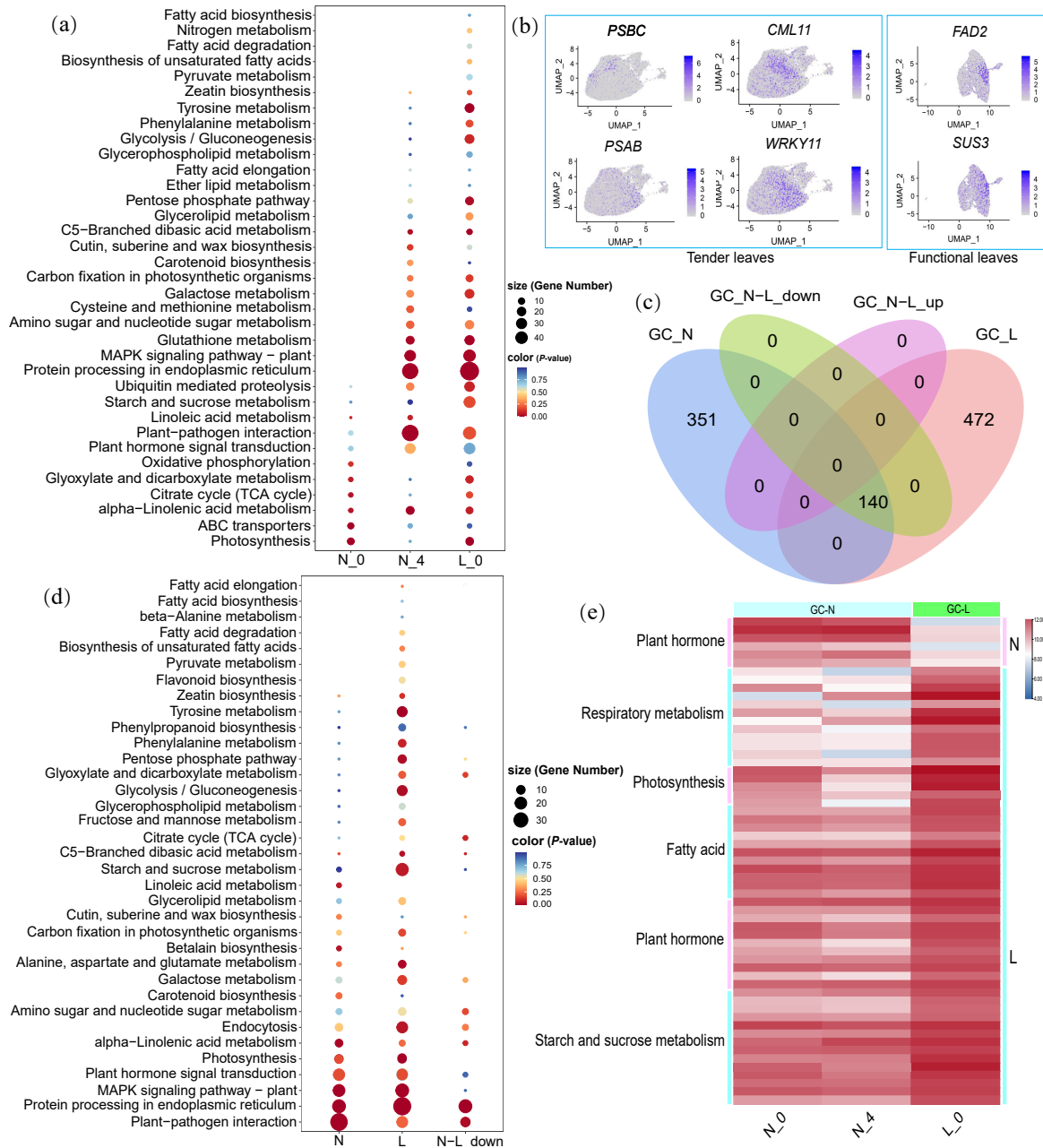


Figure 3. DEG analysis in the guard cells (GCs) of leaves at different developmental stages. (a) KEGG functional enrichment of genes in the different cell clusters of tender and functional leaves. Color (*p*-value) represents the degree of pathway enrichment; details are given in Table S13. (b) The main marker genes in the GCs of leaves at different developmental stages. (c) A Venn diagram showing the number of genes expressed in the two stages of leaf development. (d) KEGG functional enrichment analysis of these gene clusters at the two leaf developmental stages. Color (*p*-value) represents the degree of pathway enrichment; details are given in Table S14. N: genes expressed only in tender leaves; L: genes expressed only in functional leaves; N-L_down: down-regulated genes in co-expressed genes. (e) Heatmap of functional analysis of DEGs expressed separately with different expression trends in GCs of tender and functional leaves. The color bar indicates the relative expression level (red = high, blue = low).

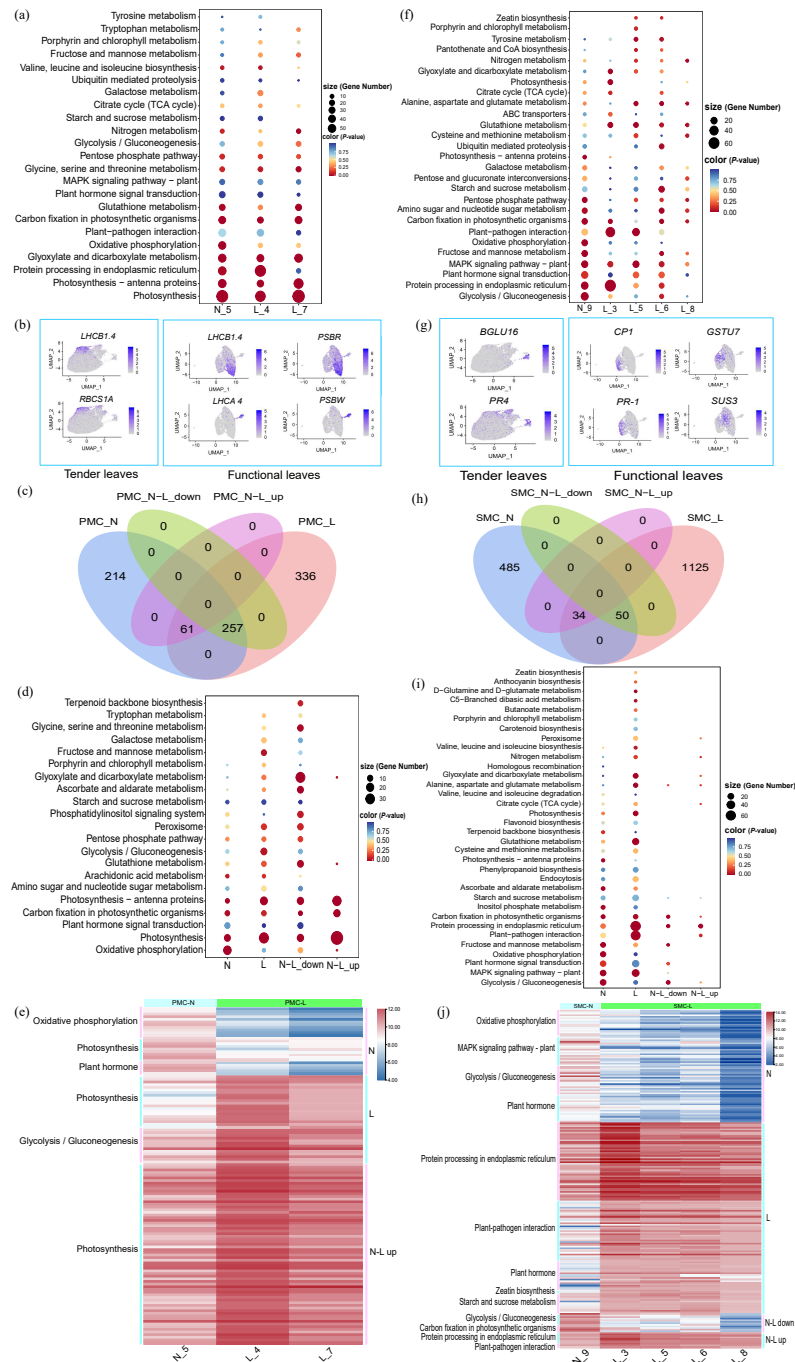


Figure 4. DEG analysis in mesophyll cells (MCs) of leaves at different developmental stages. (a,f) KEGG functional enrichment of genes in the different palisade mesophyll cell (PMC)/sponge mesophyll cell (SMC) clusters. Color (*p*-value) represents the degree of pathway enrichment; details are given in Tables S16 and S19. N: tender leaves; L: functional leaves. (b,g) The main marker genes in PMCs/SMCs at the two developmental stages. (c,h) A Venn diagram showing the number of genes expressed in PMCs/SMCs at the two stages of leaf development. (d,i) KEGG functional enrichment for four gene clusters in PMCs/SMCs at the two leaf developmental stages. Color (*p*-value) represents the degree of pathway enrichment; details are given in Table S17 and S20. N: genes expressed only in tender leaves; L: genes expressed only in functional leaves; N-L_down (up): down-regulated and up-regulated genes in co-expressed genes. (e,j) Heatmap of functional analysis of DEGs expressed separately with different expression trends in PMCs/SMCs of tender and functional leaves. The color bar indicates the relative expression level (red = high, blue = low).

Venn diagram analysis showed that 318 DEGs were co-expressed in PMCs while 214 and 336 DEGs were specifically expressed in tender and functional leaves, respectively (Figure 4c and Table S15). Genes associated with oxidative phosphorylation, photosynthesis, and carbon fixation in photosynthetic organisms were significantly expressed in the tender-leaf stage. Genes involved in pathways related to photosynthesis, glycolysis/gluconeogenesis, and carbon fixation in photosynthetic organisms were significantly expressed in the functional-leaf stage. Among the genes that were highly expressed at both stages of leaf development, those associated with photosynthesis and carbon fixation in photosynthetic organisms gradually increased with leaf development; those associated with oxidative phosphorylation, glyoxylate, and dicarboxylate metabolism gradually decreased with leaf development (Figure 4d,e and Tables S16 and S17).

3.5. Gene Expression Characteristics of Sponge Mesophyll Cells in Tender and Functional Leaves

The SMCs of tender leaves comprised Cluster 9, in which 569 DEGs were expressed. Cluster 9 was mainly enriched with genes involved in glycolysis/gluconeogenesis, oxidative phosphorylation, as well as responses to abiotic and biotic stimuli and signal response (jasmonic acid, salicylic acid, and calcium). The genes related to respiratory metabolism were *HA5* and *GAPC1*; the genes related to stress resistance were *PR3* and *WRKY FAMILY TRANSCRIPTION FACTOR (WRKY22)*. The SMCs of functional leaves comprised Clusters 3, 5, 6, and 8, in which 1204 DEGs were expressed. Clusters 3 and 5 were mainly enriched with genes related to stress resistance and respiratory metabolism, as well as a small number of genes related to photosynthesis. The genes associated with stress resistance were *CP1* and *WRKY18*, the respiratory metabolism-related genes were *RIBOSE-5-PHOSPHATE ISOMERASE 2 (RPI2)* and *HA5*, while the genes involved in photosynthesis were *PSBR* and *PHOTOSYSTEM I SUBUNIT I (PSAL)*. Clusters 6 and 8 were predominantly enriched with genes associated with stress resistance, respiratory metabolism, and starch and sucrose metabolism. The starch and sucrose metabolism-related genes were *SUS3*, *CWINV2*, and *BETA-AMYLASE 3 (BM3)*. (Figure 4f–h and Tables S3 and S4).

Venn-diagram-based analysis showed that 84 DEGs were co-expressed in SMCs while 485 and 1125 DEGs were specifically expressed in tender and functional leaves, respectively (Figure 4h and Table S18). Genes involved in glycolysis/gluconeogenesis, oxidative phosphorylation, and the MAPK signaling pathway were significantly expressed in the tender-leaf stage. Meanwhile, genes with roles in plant–pathogen interactions and photosynthesis were primarily highly expressed in the functional-leaf stage. Among the genes that were significantly expressed at both leaf development stages, those related to plant–pathogen interactions and protein processing in the endoplasmic reticulum showed a trend of increasing expression with the progression of leaf development; for those associated with glycolysis/gluconeogenesis, carbon fixation in photosynthetic organisms gradually decreased with leaf development (Figure 4i,j and Tables S19 and S20).

3.6. Gene Expression Characteristics of Vascular Cells in Tender and Functional Leaves

The VCs of tender leaves consisted of Cluster 1, in which 272 DEGs were expressed. Cluster 1 was mainly enriched with genes related to lignin biosynthesis, phloem protein, and aquaporin. The genes related to lignin biosynthesis were *PHYTOENE DESATURATION 1 (PDS1)*, *LACCASE 14 (LAC14)*, and *TYROSINE AMINOTRANSFERASE 7 (TAT7)* while the genes related to phloem protein and aquaporin were *PHLOEM PROTEIN 2-B1 (PP2-B1)*, *SEED IMBIBITION 2 (SIP2)*, and *TONOPLAST INTRINSIC PROTEIN 1;1 (TIP1;1)*. The VCs of functional leaves were composed of Clusters 1 and 9, in which 501 DEGs were expressed. Cluster 1 was principally enriched with genes related to lignin biosynthesis, phloem protein, and aquaporin. The genes related to lignin biosynthesis were *ELICITOR-ACTIVATED GENE 3-1 (ELI3-1)*, *CINNAMYL-ALCOHOL DEHYDROGENASE (CAD1)*, and *PDS1*; the genes related to phloem protein were *VEIN PATTERNING 1 (VEP1)*, *PP2-A12*, and *PP2-B1*; and the genes associated with aquaporin were *PLASMA MEMBRANE INTRINSIC PROTEIN 2A (PIP2A)*, *SIP2*, and *PLASMA MEMBRANE INTRINSIC PROTEIN 3 (SIMIP)*.

The genes in Cluster 9 were primarily associated with phloem protein and aquaporin. The top five phloem protein-related genes were PP2-A1, PP2-A10, PP2-B12, PP2-B1, and *WOODY* (*WDY*) while the aquaporin-related gene was *TIP2;1*. Cluster 9 was enriched with PP2-A1, which was found to be mainly expressed in PCCs; accordingly, Cluster 9 was classified as consisting of PCCs (Figure 5a–c and Tables S3 and S4).

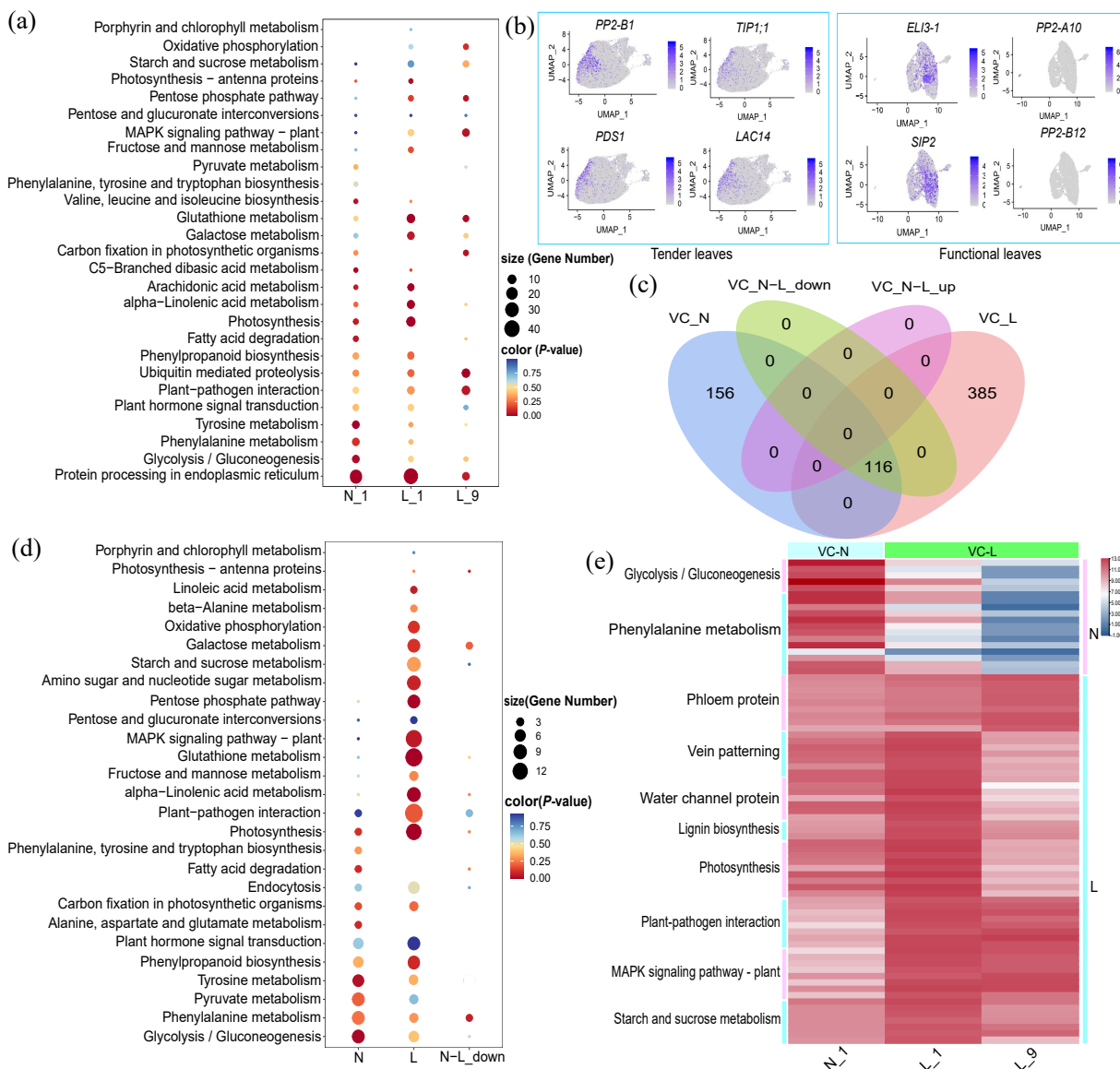


Figure 5. DEG analysis in vascular cells (VCs) of leaves at the different developmental stages. (a) KEGG functional enrichment of genes in different cell clusters of tender and functional leaves. Color (*p*-value) represents the degree of pathway enrichment; details are given in Table S22. (b) The main marker genes in VCs of leaves at the two developmental stages. (c) A Venn diagram showing the number of genes in the two stages of leaf development. (d) KEGG functional enrichment of genes in three VC clusters at the two leaf developmental stages. Color (*p*-value) represents the degree of pathway enrichment; details are given in Table S23. N: genes expressed only in tender leaves; L: genes expressed only in functional leaves; N-L_down: down-regulated genes in co-expressed genes. (e) Heatmap of functional analysis of DEGs expressed separately with different expression trends in VCs of tender and functional leaves. The color bar indicates the relative expression level (red = high, blue = low).

Venn diagram analysis indicated that 116 DEGs were co-expressed in VCs while 156 and 385 DEGs were specifically expressed in tender and functional leaves, respectively (Figure 5c and Table S21). Genes associated with phenylalanine metabolism, tyrosine metabolism, and glycolysis/gluconeogenesis were significantly expressed in the tender-leaf stage while genes related to photosynthesis and phenylpropanoid biosynthesis were significantly expressed in the functional-leaf stage. Among the genes that were significantly expressed in the two leaf developmental stages, those linked to photosynthesis, phloem protein, water channel protein, and lignin biosynthesis showed a trend of gradually increasing expression with continued leaf development. Genes related to glycolysis/gluconeogenesis and phenylalanine metabolism displayed the opposite tendency (Figure 5d,e and Tables S22 and S23).

3.7. Developmental Trajectory of Tender Leaf Cell Types

To verify the cell types and explore the continuous differentiation trajectory of leaves at different developmental stages in Poplar 84K, we first conducted a pseudo-time analysis on cells from all the clusters of the second tender leaves (Figure 6 and Table S24). The results showed that there were two branching points in the pseudo-time trajectory of tender leaves and all the cells could be divided into five states (Figure 6a). ECs and a small number of PMCs were located at the starting point of the pseudo-time differentiation trajectory (Figure 6b,c). Differentiation Trajectory 1 was divided into two parts, the completed reconstruction of GCs and a small number of VCs in State 3 and the reconstruction of PMCs and a small number of VCs in State 4. Along Differentiation Trajectory 2, the maturation of ECs and the reconstruction of GCs, SMCs, and VCs in State 5 were completed (Figure 6a,c).

The key genes related to the growth and development of tender leaves were further analyzed. Analysis of the heatmap of the pseudo-temporal distribution of the top fifty DEGs showed that the key genes in the development trajectory were divided into four subgroups and two major groups. Subgroups 1, 3, and 4 were classified as one category and Subgroup 2 as another category (Figure 6d and Table S26). The pseudo-time development starting point of Subgroups 1, 3, and 4 represents the initial stage of tender leaf development and Cluster 7 in ECs and a small number of PMCs were concentrated in this stage. The highly expressed genes were mainly the EC marker genes *HOTHEAD* (*HTH*) and *LTP1* and the cell-growth-related genes *XTH16*, *EXPL2*, and *XTH5*. The pseudo-time development endpoint of Subgroup 2 represents the terminus of tender leaf development. Clusters 2 and 3 in ECs, SMCs, GCs, and VCs were concentrated here. The highly expressed genes were primarily the EC marker genes *GLIP1* and *OPR2* and the lignin biosynthesis-related gene *O-METHYLTRANSFERASE 1* (*OMT1*) (Figure 6c,d,g).

Based on the Branch Expression Analysis Modelling (BEAM) results in Monocle 2, we detected a list of genes associated with significant changes in cell fate before and after the two branch points, mapped the cell differentiation and development trajectory of the tender leaves, and annotated the highly expressed genes in each state and branching point (Figure 6e,f and Table S18). At Branch Point 1, the genes showing significant expression changes were divided into four subgroups and two major groups, with Subgroups 1–3 comprising one category and Subgroup 4 another. In the initial stage of Subgroups 1–3, which mainly consisted of Clusters 6 and 7 of ECs and a small number of PMCs, the highly expressed genes were mainly associated with cell growth and photosynthesis (Figure 6c,e,h), indicating that tender leaf cells in State 1 had strong differentiation ability (Figure 6a). When cells in States 1 and 2 differentiated into State-4 cells, the expression of genes in Subgroups 1–3 that were related to photosynthesis and lignin biosynthesis and metabolism gradually increased, indicating that cells in State 1 gradually differentiated into PMCs and VCs in State 4. Genes related to photosynthesis (*LHCB1.4*, *PSBW*, *PSI-H*) and carbon metabolism (*RBCS1A*) were specifically highly expressed in PMCs while the lignin biosynthesis gene *PHE AMMONIA LYASE 1* (*PAL1*) and the gene *TIP1;1*, encoding a water channel protein, were specifically highly expressed in VCs (Figure 6e). When cells in States 1 and 2 differentiated into State-3 cells, the expression levels of genes in Subgroup

4 that were related to respiratory metabolism, such as *HA5* and *SU(VAR)3-9 HOMOLOG 5 (SUVH5)*, and the stomata-specific expression gene *MPK3* gradually increased to State 3, indicating that cells in State 1 gradually differentiated into State-3 GCs (Figure 6e). At Branch Point 2, the genes exhibiting significant expression changes were divided into four subgroups and two major groups, with Subgroup 3 comprising one category and Subgroups 1, 2, and 4 comprising another. ECs in State 1 mainly comprised Clusters 6 and 7. At the starting point of Subgroups 1 and 2, highly expressed genes were involved with genes related to cell growth, such as *EXPL2* and *AUXIN RESPONSES FACTOR 15 (ARF15)*. When cells differentiated along Branch Point 2 to EC Clusters 2, 3, 6, and 8 in State 5, the expression of genes related to cell growth was downregulated. Meanwhile, the genes that were highly expressed in ECs of the development terminus included the fatty acid metabolism-related genes *ChlAKR* and *OPR2*. These observations indicated that ECs had completed the transition from a state with high differentiation potential to a state of functional maturity (Figure 6f,i). Combined, these results demonstrated that tender leaves begin the cytogenesis process as ECs, which subsequently differentiate into different cell types by expressing different functional genes, finally completing the process of cell functional differentiation.

3.8. Developmental Trajectory of Functional Leaf Cell Types

To further explore the processes involved in leaf development, we conducted a pseudo-time analysis on cells from all the clusters of the fifth functional leaves (Figure 7 and Table S25). The results showed that there were two branching points in the pseudo-time trajectory of functional leaves and all the cells were divided into five states (Figure 7a). ECs, GCs, SMCs, and PCCs were located at the starting point of the pseudo-time differentiation trajectory (Figure 7b,c). Differentiation Trajectory 1 was divided into two parts, in which SMCs and some VCs in State 3 completed their transition to maturity, as did PMCs, VCs, and GCs in States 1, 2, and 5. Differentiation Trajectory 2 was also divided into two parts, which involved the establishment of PMCs and the transition of VCs in State 1 and the transition of State-5 GCs and VCs to maturity (Figure 7a,c).

The key genes related to the growth and development of functional leaves were further analyzed. Analysis of the heatmap of the pseudo-temporal distribution of the top fifty DEGs showed that the key genes in the functional leaf development trajectory were divided into four subgroups and two major groups, with Subgroups 1 and 2 classified as one category and Subgroups 3 and 4 as another (Figure 7d and Table S17). The pseudo-time developmental starting points for Subgroups 1 and 2 represented the initial stage; ECs and SMC Clusters 5, 6, and 8 were concentrated in this stage (Figure 7c,d). The highly expressed genes were the unsaturated fatty acid biosynthesis genes *FAD2* and *OPR2* and the respiratory metabolism-related genes *HA5* and *ACO3*. The pseudo-time developmental endpoint of Subgroups 3 and 4 represented the terminus of functional leaf development and PMCs and VCs were the most abundant cell types at this stage (Figure 7c,d). The highly expressed genes were primarily involved in the photosynthesis genes *PSBR*, *LHCB1.4*, and *RBCS1A* and lignin biosynthesis-related genes *PAL1* and *ELI3-1*. These genes were upregulated as leaf development progressed (Figure 7d,g).

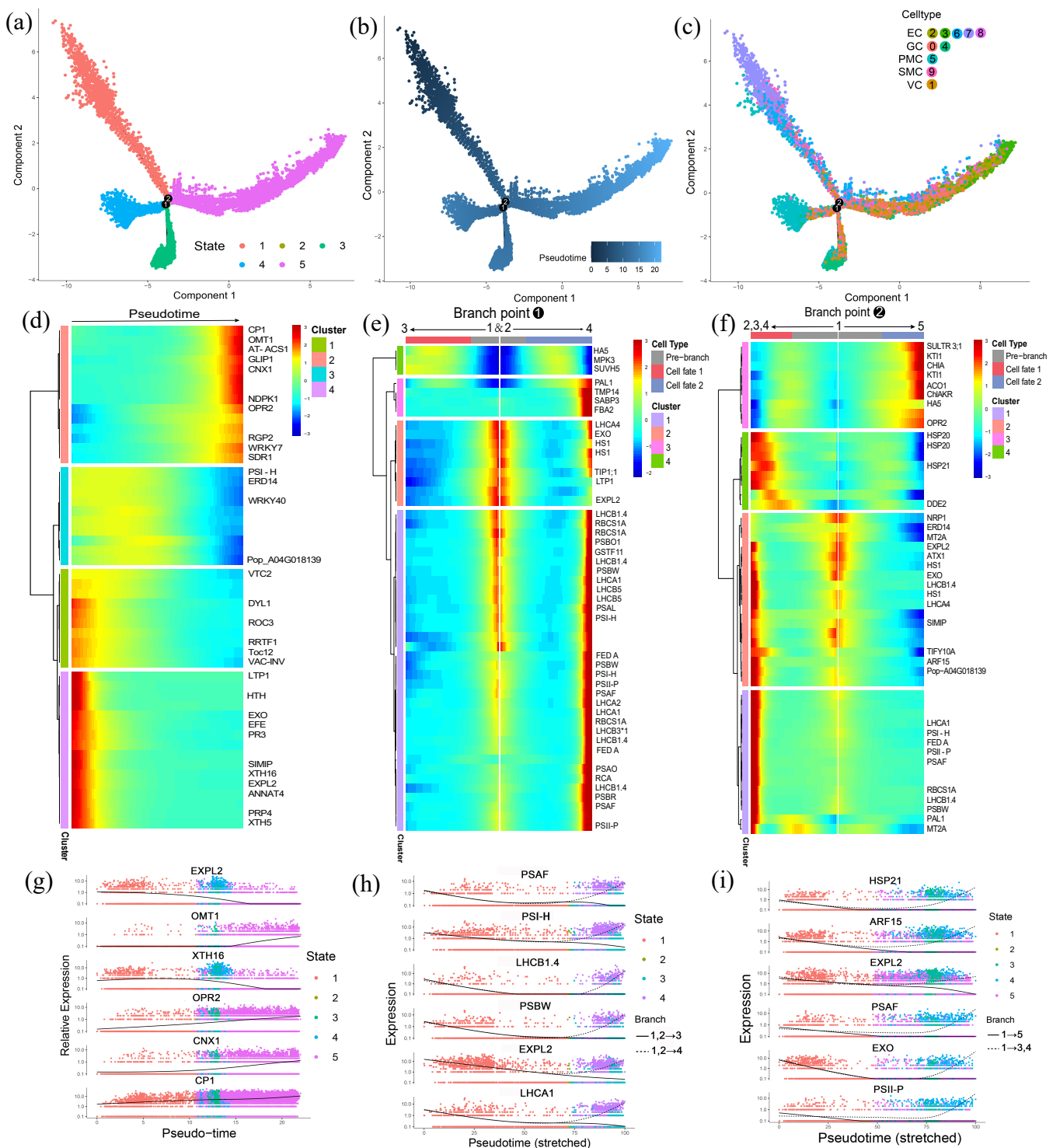


Figure 6. Construction of a tender leaf development trajectory for Poplar 84K. (a–c) Cell ordering along the differentiation trajectory is successively presented by state, pseudo-time, and cell type. (d) Heatmap of the changes in the distribution of the top fifty DEGs among the five cell states. The description of these genes is given in Table S26. The color bar indicates the relative expression level (red = high, blue = low). (e,f) Heatmap of the top fifty DEGs in the two branch points identified using the BEAM function in Monocle 2. Details of these genes are given in Table S28. The color bar indicates the relative expression level (red = high, blue = low). (g) Representative genes of the five cell states. (h,i) The expression trends of representative genes of the two branch points before and after cell differentiation.

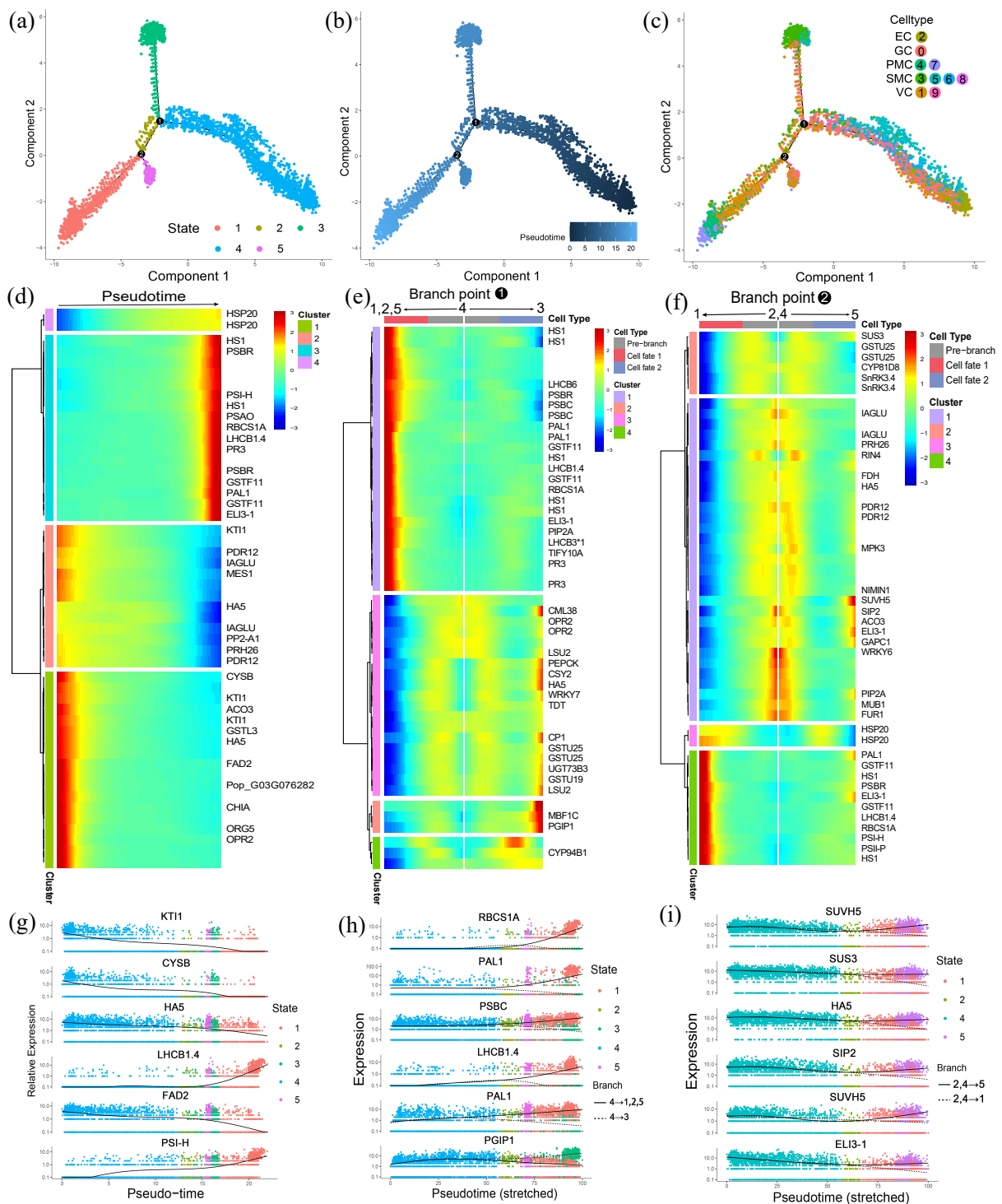


Figure 7. Construction of a functional leaf development trajectory for Poplar 84K. (a–c) Cell ordering along the differentiation trajectory is successively presented by state, pseudo-time, and cell type. (d) Heatmap of the changes in the distribution of the top fifty DEGs among the five cell states. The description of these genes is given in Table S27. The color bar indicates the relative expression level (red = high, blue = low). (e,f) Heatmap of the top fifty DEGs in the two branch points identified using the Branch BEAM function in Monocle 2. Details of these genes are given in Table S29. The color bar indicates the relative expression level (red = high, blue = low). (g) Representative genes of the five cell states. (h,i) The expression trends of representative genes of the two branch points before and after cell differentiation.

Based on the BEAM results from Monocle 2, we detected a list of genes associated with significant changes in cell fate before and after the two branch points, mapped the cell differentiation and development trajectory of the functional leaves, and annotated the highly expressed genes in each state and branching point (Figure 7e,f and Table S19). At Branch Point 1, the genes displaying significant changes in expression were divided into four subgroups and two categories. Subgroups 2–4 comprised one category and Subgroup 1 comprised another. Functional leaves in State 4 mainly contained ECs and SMC Clusters 5, 6, and 8. In the initial stage, the highly expressed genes in Subgroups 2–4 were mainly EC marker genes and genes related to stress resistance (Figure 7e,h). As cells in State 4 differentiated into State-3 cells, the expression of the respiratory metabolism-related genes *HA5* and *CITRATE SYNTHASE 2 (CSY2)* and that of the response to the abiotic and biological stimuli-related genes *CML38* and *CP1* in Subgroups 2–4 were gradually upregulated. It was shown that the cells in State 4 gradually transitioned to State 3 to Clusters 3 and 5 of mature SMCs and a small number of GCs (Figure 7e). When cells in State 4 differentiated into cells in States 1, 2, and 5, the expression levels of genes related to photosynthesis (*LHCB1.4*, *PSBR*, and *PSBC*), carbon metabolism (*RBCS1A*), lignin synthesis (*PAL1* and *ELI3-1*), and aquaporin (*PIP2A*) in Subgroup 1 gradually increased, indicating that the cells in State 4 gradually differentiated into PMCs, VCs, and GCs in States 1, 2, and 5 (Figure 7e). At Branch Point 2, genes displaying significant changes in expression were divided into four subgroups and two categories, with Subgroups 1 and 2 constituting one category and Subgroups 3 and 4 constituting another (Figure 7f). States 2 and 4 mainly included ECs, GCs, SMCs, and PCCs. The genes in Subgroups 1 and 2 that were highly expressed at the initial stage of differentiation mainly included *HA5* and *ACO3*, which are involved in respiratory metabolism; *ELI3-1*, which plays a role in lignin biosynthesis; *PIP2A* and *SIP2*, which are associated with aquaporin; and the stomatal marker gene *MPK3* (Figure 7f,i). When cells in States 2 and 4 differentiated into State-5 cells, the expression levels of these highly expressed genes first decreased and, then, gradually increased with continued functional leaf development, indicating that GCs and VCs gradually transitioned to a mature state as leaf development progressed. When cells in States 2 and 4 differentiated into State-1 cells, genes in Subgroups 3 and 4 that were highly expressed at the terminus of functional leaf development primarily included *PSBR*, *LHCB1.4*, and *PHOTOSYSTEM II SUBUNIT P (PSII-P)*, which are related to photosynthesis; *RBCS1A*, which is involved in carbon metabolism; and *PAL1* and *ELI3-1*, which play a role in lignin biosynthesis, indicating that the terminus of leaf development involved PMC formation and the transition of VCs to a mature state (Figure 7f). These results demonstrated that functional leaf cells had completed their maturation and the establishment of different cell types through the expression of different functional genes and the leaves had entered the initial formation stage of photosynthesis.

The results of the pseudo-time analysis showed that all cells could be arranged along a major developmental trajectory. The tender second leaf and the functional fifth leaf represented two different developmental stages. The pseudo-time trajectory analysis of tender leaves at the second leaf position showed that Clusters 6 and 7 in ECs were the earliest cell types in development with strong cell differentiation ability, indicating that there was active cell division in the ECs of tender leaves. Along the pseudo-time differentiation trajectory, according to the differentiation of different cell functions, SMCs, GCs, VCs, a small number of PMCs, and more mature ECs (Clusters 2,3,6 and 8) were eventually developed. With the growth and development of leaves, the leaf surface area of the functional leaf at the fifth leaf position increased to the maximum. The pseudo-time trajectory analysis showed that ECs and SMCs were located at the starting point of the trajectory and were the earliest-developed cell types. With the further maturation of the leaves, the expression of genes related to photosynthesis, lignin biosynthesis, and aquaporins was significantly up-regulated, indicating that the PMCs and SMCs of the leaves matured, mesophyll cells became the most important cell type in the leaves, and the photosynthetic products by photosynthesis became the main source of the growth of leaves

and the whole plant. The development of VCs was also more mature so that the veins were responsible for supporting the leaves and could play a good role in transporting water and photosynthetic products.

4. Discussion

4.1. Transcriptome Differences among Leaf Cell Types at Different Developmental Stages at the Single-Cell Level

The identity and function of plant cells are largely influenced by their precise location within the plant body. Therefore, to understand plant development at the molecular level, it is necessary not only to characterize the molecular status of each cell but also to know their cell type and physical location in the plant [51]. ScRNA-seq can be used to classify plant tissue cells at the single-cell level [22,30,52]. In Arabidopsis, mature leaf cells were divided into nineteen distinct clusters and five cell types were identified—mesophyll, epidermal, guard, hydathode, and vascular cells [30]. In this study, we undertook a comparative analysis of the cell atlases of the tender and functional leaves of Poplar 84K. Finally, tender leaves were divided into five cell types—ECs, GCs, PMCs, SMCs, and VCs. Similarly, functional leaves were divided into six cell types, namely, ECs, GCs, PMCs, SMCs, VCs, and PCCs.

GO and KEGG analyses of genes specifically expressed in different cell types can provide an in-depth and systematic study of the differences in biological function among different cell types [20]. The results of this study showed that there were significant differences in biological function among different cell types during different developmental stages of Poplar 84K. Among them, ECs of tender and functional leaves were enriched with genes related to fatty acid biosynthesis and metabolism pathways [11,14,22]. At the tender-leaf stage, ECs were the main cell type and were enriched with genes related to fatty acid biosynthesis and metabolism, respiratory metabolism, stress resistance, cell growth, cell expansion, and auxin [53]. With the development of leaves, the expression of genes related to fatty acid biosynthesis was downregulated and unsaturated fatty acid biosynthesis and stress resistance were upregulated in the functional-leaf stage, indicating that ECs of functional leaves formed mature cuticles [6,54,55], which could better protect the mesophyll cell layer from direct physical damage. Concomitantly, the expression of genes related to cell growth, cell expansion, and auxin was strongly downregulated in functional leaf ECs, indicating that tender leaf ECs had high differentiation ability. Primary epidermal cells differentiate into specialized stomatal guard cells via a series of asymmetric divisions [9,19,56,57]; guard cells are specialized cells in epidermal cells. The results of this study showed that GCs of tender leaves were mainly enriched with genes related to fatty acid biosynthesis, respiratory metabolism, and photosynthesis. With the development of leaves, the expression of genes associated with unsaturated fatty acid and fatty acid biosynthesis, respiratory metabolism, and stress resistance were upregulated by the functional-leaf stage, indicating that the development of GCs and ECs was consistent and mature GCs can play a protective role in the mesophyll cell layer. Simultaneously, the expressions of genes related to starch and sucrose metabolism and photosynthesis were upregulated in the functional-leaf stage, suggesting that photosynthesis and starch–sugar transformations are necessary for regulating mature-guard-cell-mediated stomatal opening and closing [58]. Mesophyll cells are the main sites of photosynthesis in leaves. In the single-cell transcriptome of young leaves of Chinese cabbage, crantz, and tea plants, it was found that the abundance of photosynthesis-related genes was highest in PMCs [6,10,12,14]. The results of this study showed that PMCs of tender leaves were mainly enriched with genes involved in photosynthesis and carbon assimilation. With the development of leaves, the number and the expression levels of these genes in the functional-leaf stage were significantly upregulated. This suggested that PMCs were the main site of photosynthesis and the photosynthesis and carbon assimilation ability began to increase at the functional leaf development stage; the leaf morphogenesis had been completed. Leaf veins contain a highly specialized vascular system composed of xylem and phloem cells [20,25]. Our

results showed that tender and functional leaves were enriched with xylem and phloem marker genes [12]; however, there were significant differences in gene expression. VCs of tender leaves were enriched with genes related to lignin biosynthesis, phloem protein, and aquaporin. The expression of genes related to lignin biosynthesis was upregulated in VCs at the functional-leaf stage and there was an enrichment of genes related to phloem proteins and aquaporins in VCs with continued leaf development, indicating that VCs at this stage were more mature. Mature VCs play a key role in transporting water, inorganic salts, and organic nutrients and also afford mechanical support [14]. These results provide a theoretical basis for further understanding plant leaf growth and development.

4.2. Cell Differentiation Trajectory and Gene Expression Characteristics of Tender Leaves

The construction of leaf cell differentiation trajectories based on scRNA-seq data is beneficial for better-describing leaf cell development. The development of plant leaves to their final morphology requires cell proliferation and cell expansion, with cell expansion making a significant contribution to the final leaf size [14,59,60]. In a study involving a pseudo-time trajectory analysis of peanut tender leaves, it was found that epidermal cells developed earlier than primordial cells [3]. In our study, we found that ECs were the first cells to develop in tender leaves. At the initial stages of development, EC Clusters 6 and 7 were enriched with genes related to cell growth and cell expansion, such as *EXPL2*, *XTH16*, *XTH5*, and *ARF15* [59,61–63]. Additionally, the expression levels of these genes gradually decreased with leaf development, indicating that EC Clusters 6 and 7 had high differentiation ability. At the same time, with EC Clusters 6 and 7 as the starting point of development, along the pseudo-time differentiation trajectory, cells showing a gradual increase in the expression of genes related to photosynthesis and carbon metabolism developed into PMCs; cells exhibiting an increase in the expression of genes related to plant respiratory metabolism and responses to abiotic and biological stimuli and signal responses developed into SMCs; cells displaying an increased expression of genes associated with respiratory metabolism and stomatal-specific expression developed into GCs; cells with increasing expression of genes linked to lignin biosynthesis, phloem protein, and aquaporin developed into VCs; and cells in which the expression levels of genes related to fatty acid biosynthesis and metabolism were transformed into more mature Cluster 2, 3, 6, and 8 ECs, thereby completing the functional differentiation of tender leaf cells. The development of tender leaves begins in some ECs, which, via the expression of different functional genes, subsequently give rise to populations of different cell types with different functions. This indicates that tender leaves are in a stage of cell expansion and functional differentiation.

4.3. Cell Differentiation Trajectory and Gene Expression Characteristics of Functional Leaves

Leaf development is a continuous process that is accompanied by significant changes in the transcriptome profile, metabolism, and cell morphology [20]. After the period of cell expansion and functional differentiation, the leaves had completed morphogenesis and their photosynthetic capacity was enhanced [64]. In a pseudo-time study involving cassava leaves, it was found that genes that were highly expressed in the branches of PMCs were mainly related to photosynthesis [14]. In this study, we found that ECs and SMCs were located at the starting point of the pseudo-time differentiation trajectory of functional leaves. With continued leaf development, genes related to photosynthesis, such as *PSBR* [65], *PSI-H* [66], and *LHCBI.4* [6,10,11], and the gene *RBCS1A*, which is associated with carbon metabolism [20,22], were strongly upregulated, indicating that leaf development had entered the initial formative stage of photosynthesis. During this period, along the pseudo-time trajectory, SMCs gradually transitioned to a more mature state and genes involved in respiratory metabolism and stress-related pathways became more abundant. VCs also progressed into a mature state, characterized by an abundance of lignin biosynthesis genes and the upregulation of the expression of aquaporin-related genes. When leaves reached the functional-leaf stage, we found that PMCs were the main photosynthetic sites in leaves and their photosynthetic functions and carbon metabolism

were significantly enhanced, indicating that functional leaves were in the initial stage of leaf development and photosynthesis formation.

4.4. Temporal Transcriptome Changes between Cell Types in Tender and Functional Leaves

The expression of genes involved in leaf development showed a temporal pattern. In poplar, leaf development can be divided into five stages—young leaf cell genesis and functional differentiation, young leaf development and the initial formation of photosynthetic capacity, the period of maximum photosynthetic capacity of functional leaves, the period of decreasing photosynthetic capacity of functional leaves, and the period of senescent leaves [64]. The leaves used in this study were in the stage of leaf cell expansion and functional differentiation and the initial formation of leaf development and photosynthetic capacity. ECs at the tender-leaf stage exhibited the highest expression levels of genes related to cell division, cell growth, and hormones, such as auxin, cytokinin, and brassinosteroid. At this time, the leaves were in the stage of cell expansion and functional differentiation. When leaves reached the functional-leaf stage, EC clusters underwent continuous development and functional differentiation, leaving only one EC cluster, and the expression of genes related to cell division and growth functions gradually decreased. Meanwhile, the different cell types transitioned into a more mature state. At this time, mesophyll cells had the largest number of cell clusters and the abundance and expression levels of genes involved in photosynthesis and carbon metabolism began to increase significantly. This indicated that leaf morphogenesis was completed at this stage and that the photosynthetic capacity of the leaves was enhanced. The leaves in this period were in the stage of leaf development and the initial formation of photosynthesis capacity. A more in-depth analysis of the phased changes in the expression levels of genes that occur during Poplar 84K leaf development will help us to understand the regulation mechanism of development genes in different cell types of leaves and will contribute to improving the photosynthetic carbon assimilation ability of leaves through genetic improvements.

5. Conclusions

In this study, we applied scRNA-seq technology to the Poplar 84K leaves at different developmental stages and found that they were composed of highly heterogeneous cells. Using a series of new cell-type-specific marker genes, we identified ten distinct cell clusters and five cell types in tender leaves. A total of ten distinct cell clusters and six cell types were identified in the functional leaves. Furthermore, the cell differentiation trajectories of the leaves at different developmental stages were constructed using the expression dynamics of these marker genes. In summary, our study established a transcriptome atlas of the main cell types of leaves at different developmental stages of Poplar 84K under a single-cell-level resolution. The results provide valuable resources for the gene expression and functional analyses of poplar leaf development and act as a basis for future molecular breeding research on poplar.

Supplementary Materials: The following supporting information can be downloaded at: <https://www.mdpi.com/article/10.3390/f15030512/s1>, Figure S1: Data quality control and data filtering. Figure S2: Gene ontology (GO) analysis of DEGs in tender leaves. Figure S3: GO analysis of DEGs in functional leaves. Figure S4: Kyoto Encyclopedia of Genes and Genomes (KEGG) analysis of enriched pathways among DEGs in tender leaves. Figure S5: KEGG analysis of enriched pathways among DEGs in functional leaves. Figure S6: Top10 marker gene clustering heat map of different cell clusters in tender leaves. Figure S7: Top10 marker gene clustering heat map of different cell clusters in functional leaves. Figure S8: Top10 marker gene clustering heat map of different cell clusters in tender leaves. Figure S9: Top10 marker gene clustering heat map of different cell clusters in functional leaves. Table S1: Statistical data of scRNA-seq. Table S2: List of poplar cell type-specific marker genes, generated by evaluating the expression of poplar. Table S3: Marker genes list of tender leaves cell Clusters 0 to 9. Table S4: Marker genes list of functional leaves cell Clusters 0 to 9. Table S5: Gene ontology (GO) annotation list of functional leaf differentially expressed genes (DEGs). Table S6: GO annotation list of tender leaf DEGs. Table S7: Kyoto Encyclopedia of Genes and Genomes (KEGG)

annotation list of functional leaf DEGs. Table S8: KEGG annotation list of tender leaf DEGs. Table S9: DEGs list of leaf epidermal cells (ECs) at different developmental stages. Table S10: KEGG functional enrichment of genes in different cell clusters of tender and functional leaves ECs. Table S11: KEGG functional enrichment analysis of four gene clusters at two leaf developmental stages ECs. Table S12: DEGs list of stomatal guard cells (GCs) in leaves of poplar at different developmental stages. Table S13: KEGG functional enrichment of genes in different cell clusters of tender and functional leaves GCs. Table S14: KEGG functional enrichment analysis of three gene clusters at two leaf developmental stages GCs. Table S15: DEGs list of leaf palisade mesophyll cells (PMCs) at different developmental stages. Table S16: KEGG functional enrichment of genes in different cell clusters of tender and functional leaves PMCs. Table S17: KEGG functional enrichment analysis of four gene clusters at two leaf developmental stages PMCs. Table S18: DEGs list of leaf sponge mesophyll cells (SMCs) at different developmental stages. Table S19: KEGG functional enrichment of genes in different cell clusters of tender and functional leaves SMCs. Table S20: KEGG functional enrichment analysis of four gene clusters at two leaf developmental stages SMCs. Table S21: DEGs list of leaf vascular cells (VCs) at different developmental stages. Table S22: KEGG functional enrichment of genes in different cell clusters of tender and functional leaves VCs. Table S23: KEGG functional enrichment analysis of three gene clusters at two leaf developmental stages VCs. Table S24: Determination of pseudo-time differentiation trajectory timeline of tender leaves. Table S25: Determination of pseudo-time differentiation trajectory timeline of functional leaves. Table S26: Top 50 genes of pseudotime analysis of tender leaves. Table S27: Top 50 genes of pseudotime analysis of functional leaves. Table S28: The top 50 significantly changed genes discovered by the Branch Expression Analysis Modelling (BEAM) of 2 differentiation trajectory branch points of tender leaves. Table S29: The top 50 significantly changed genes discovered by the BEAM of 2 differentiation trajectory branch points of functional leaves.

Author Contributions: X.K. and Y.J. conceived the project; Y.J. and Y.R. designed and performed the experiments; Y.J. and S.Z. analyzed the data; Y.J. and X.K. participated in the discussion of the results; Y.J. wrote the manuscript; Y.J. and X.K. wrote, reviewed, and edited the manuscript. All authors have read and agreed to the published version of the manuscript.

Funding: This research was funded by the National Key R&D Program of China during the 14th Five-year Plan Period (2021YFD2200105).

Data Availability Statement: All data supporting the findings of this study are available within the paper and its Supplementary Materials published online.

Conflicts of Interest: The authors declare no conflicts of interest.

Abbreviations

scRNA-seq	Single-cell RNA sequencing
MS	Murashige and Skoog (1962)
NAA	1-Naphthaleneacetic acid
IBA	Indole butyric acid
MES	2-(N-morpholino) ethanesulfonic acid hydrate
BSA	Bovine serum albumin
FDA	Fluorescein diacetate
cDNA	Complementary DNA
GEM	10x Genomics Gel in Emulsion
PCA	Principal component analysis
UMAP	Uniform manifold approximation and projection
PCs	Principal components
DEGs	Differentially expressed genes
PCMDB	Plant cell marker database
GO	Gene ontology
KEGG	Kyoto encyclopedia of genes and genomes
BEAM	Branch expression analysis modeling

References

- Urry, L.A.; Cain, M.L.; Wasserman, S.A.; Minorsky, P.V.; Reece, J.B. *Campbell Biology*, 11th ed.; Pearson: New York, NY, USA, 2016; pp. 9–11.
- Taiz, L.; Zeiger, E. *Plant Physiology*, 5th ed.; Sinauer Associates: New York, NY, USA, 2015; pp. 52–64.
- Liu, H.; Hu, D.; Du, P.; Wang, L.; Liang, X.; Li, H.; Lu, Q.; Li, S.; Liu, H.; Chen, X.; et al. Single-cell RNA-seq describes the transcriptome landscape and identifies critical transcription factors in the leaf blade of the allotetraploid peanut (*Arachis hypogaea* L.). *Plant Biotechnol. J.* **2021**, *19*, 2261–2276. [[CrossRef](#)] [[PubMed](#)]
- Denyer, T.; Ma, X.; Klesen, S.; Scacchi, E.; Nieselt, K.; Timmermans, M.C.P. Spatiotemporal Developmental Trajectories in the *Arabidopsis* Root Revealed Using High-Throughput Single-Cell RNA Sequencing. *Dev. Cell* **2019**, *48*, 840–852. [[CrossRef](#)] [[PubMed](#)]
- Jean-Baptiste, K.; McFaline-Figueroa, J.L.; Alexandre, C.M.; Dorrity, M.W.; Saunders, L.; Bubb, K.L.; Trapnell, C.; Fields, S.; Queitsch, C.; Cuperus, J.T. Dynamics of Gene Expression in Single Root Cells of *Arabidopsis thaliana*. *Plant Cell* **2019**, *31*, 993–1011. [[CrossRef](#)]
- Procko, C.; Lee, T.; Borsuk, A.; Bargmann, B.; Dabi, T.; Nery, J.R.; Estelle, M.; Baird, L.; O'Connor, C.; Brodersen, C.; et al. Leaf cell-specific and single-cell transcriptional profiling reveals a role for the palisade layer in UV light protection. *Plant Cell* **2022**, *34*, 3261–3279. [[CrossRef](#)]
- Zhang, T.Q.; Xu, Z.G.; Shang, G.D.; Wang, J.W. A Single-Cell RNA Sequencing Profiles the Developmental Landscape of *Arabidopsis* Root. *Mol. Plant* **2019**, *12*, 648–660. [[CrossRef](#)]
- Brady, S.M.; Orlando, D.A.; Lee, J.; Wang, J.Y.; Koch, J.; Dinneny, J.R.; Mace, D.; Ohler, U.; Benfey, P.N. A high-resolution root spatiotemporal map reveals dominant expression patterns. *Science* **2007**, *318*, 801–806. [[CrossRef](#)]
- Xia, K.; Sun, H.X.; Li, J.; Li, J.; Zhao, Y.; Chen, L.; Qin, C.; Chen, R.; Chen, Z.; Liu, G.; et al. The single-cell stereo-seq reveals region-specific cell subtypes and transcriptome profiling in *Arabidopsis* leaves. *Dev. Cell* **2022**, *57*, 1299–1310. [[CrossRef](#)]
- Guo, X.; Liang, J.; Lin, R.; Zhang, L.; Zhang, Z.; Wu, J.; Wang, X. Single-cell transcriptome reveals differentiation between adaxial and abaxial mesophyll cells in *Brassica rapa*. *Plant Biotechnol. J.* **2022**, *20*, 2233–2235. [[CrossRef](#)]
- Tenorio, B.R.; Verstaen, K.; Vandamme, N.; Pevernagie, J.; Achon, I.; Van Duyse, J.; Van Isterdael, G.; Saeys, Y.; De Veylder, L.; Inze, D.; et al. Single-cell transcriptomics sheds light on the identity and metabolism of developing leaf cells. *Plant Physiol.* **2022**, *188*, 898–918. [[CrossRef](#)] [[PubMed](#)]
- Wang, Q.; Wu, Y.; Peng, A.; Cui, J.; Zhao, M.; Pan, Y.; Zhang, M.; Tian, K.; Schwab, W.; Song, C. Single-cell transcriptome atlas reveals developmental trajectories and a novel metabolic pathway of catechin esters in tea leaves. *Plant Biotechnol. J.* **2022**, *20*, 2089–2106. [[CrossRef](#)] [[PubMed](#)]
- Wang, Y.; Huan, Q.; Li, K.; Qian, W. Single-cell transcriptome atlas of the leaf and root of rice seedlings. *J. Genet. Genom.* **2021**, *48*, 881–898. [[CrossRef](#)]
- Zang, Y.; Pei, Y.; Cong, X.; Ran, F.; Liu, L.; Wang, C.; Wang, D.; Min, Y. Single-cell RNA sequencing profiles reveal the developmental landscape of *Manihot esculenta* Crantz leaves. *Plant Physiol.* **2023**, *194*, 456–474. [[CrossRef](#)] [[PubMed](#)]
- Cheng, Z.; Mu, C.; Li, X.; Cheng, W.; Cai, M.; Wu, C.; Jiang, J.; Fang, H.; Bai, Y.; Zheng, H.; et al. Single-cell transcriptome atlas reveals spatiotemporal developmental trajectories in the basal roots of moso bamboo (*Phyllostachys edulis*). *Hortic. Res.* **2023**, *10*, uhad122. [[CrossRef](#)] [[PubMed](#)]
- Shahan, R.; Hsu, C.; Nolan, T.M.; Cole, B.J.; Taylor, I.W.; Greenstreet, L.; Zhang, S.; Afanassiev, A.; Vlot, A.H.C.; Schiebinger, G.; et al. A single-cell *Arabidopsis* root atlas reveals developmental trajectories in wild-type and cell identity mutants. *Dev. Cell.* **2022**, *57*, 543–560. [[CrossRef](#)] [[PubMed](#)]
- Zhang, L.; He, C.; Lai, Y.; Wang, Y.; Kang, L.; Liu, A.; Lan, C.; Su, H.; Gao, Y.; Li, Z.; et al. Asymmetric gene expression and cell-type-specific regulatory networks in the root of bread wheat revealed by single-cell multi omics analysis. *Genome Biol.* **2023**, *24*, 65. [[CrossRef](#)] [[PubMed](#)]
- Shulse, C.N.; Cole, B.J.; Ciobanu, D.; Lin, J.; Yoshinaga, Y.; Gouran, M.; Turco, G.M.; Zhu, Y.; O'Malley, R.C.; Brady, S.M.; et al. High-Throughput Single-Cell Transcriptome Profiling of Plant Cell Types. *Cell Rep.* **2019**, *27*, 2241–2247. [[CrossRef](#)] [[PubMed](#)]
- Zhang, T.Q.; Chen, Y.; Wang, J.W. A single-cell analysis of the *Arabidopsis* vegetative shoot apex. *Dev. Cell* **2021**, *56*, 1056–1074. [[CrossRef](#)] [[PubMed](#)]
- Liu, Z.; Wang, J.; Zhou, Y.; Zhang, Y.; Qin, A.; Yu, X.; Zhao, Z.; Wu, R.; Guo, C.; Bawa, G.; et al. Identification of novel regulators required for early development of vein pattern in the cotyledons by single-cell RNA-sequencing. *Plant J.* **2022**, *110*, 7–22. [[CrossRef](#)] [[PubMed](#)]
- Liu, Z.; Zhou, Y.; Guo, J.; Li, J.; Tian, Z.; Zhu, Z.; Wang, J.; Wu, R.; Zhang, B.; Hu, Y.; et al. Global Dynamic Molecular Profiling of Stomatal Lineage Cell Development by Single-Cell RNA Sequencing. *Mol. Plant* **2020**, *13*, 1178–1193. [[CrossRef](#)]
- Sun, Y.; Han, Y.; Sheng, K.; Yang, P.; Cao, Y.; Li, H.; Zhu, Q.H.; Chen, J.; Zhu, S.; Zhao, T. Single-cell transcriptomic analysis reveals the developmental trajectory and transcriptional regulatory networks of pigment glands in *Gossypium bickii*. *Mol. Plant* **2023**, *16*, 694–708. [[CrossRef](#)]
- Xie, J.B.; Li, M.; Zeng, J.Y.; Li, X.; Zhang, D.Q. Single-cell RNA sequencing profiles of stem-differentiating xylem in poplar. *Plant Biotechnol. J.* **2022**, *20*, 417–419. [[CrossRef](#)] [[PubMed](#)]
- Li, H.; Dai, X.; Huang, X.; Xu, M.; Wang, Q.; Yan, X.; Sederoff, R.R.; Li, Q. Single-cell RNA sequencing reveals a high-resolution cell atlas of xylem in *Populus*. *J. Integr. Plant Biol.* **2021**, *63*, 1906–1921. [[CrossRef](#)] [[PubMed](#)]

25. Chen, Y.; Tong, S.; Jiang, Y.; Ai, F.; Feng, Y.; Zhang, J.; Gong, J.; Qin, J.; Zhang, Y.; Zhu, Y.; et al. Transcriptional landscape of highly lignified poplar stems at single-cell resolution. *Genome Biol.* **2021**, *22*, 319. [[CrossRef](#)]
26. Roszak, P.; Heo, J.; Blob, B.; Toyokura, K.; Sugiyama, Y.; de Luis Balaguer, M.A.; Lau, W.W.Y.; Hamey, F.; Cirrone, J.; Madej, E.; et al. Cell-by-cell dissection of phloem development links a maturation gradient to cell specialization. *Science* **2021**, *374*, eaba5531. [[CrossRef](#)]
27. Ichino, L.; Picard, C.L.; Yun, J.; Chotai, M.; Wang, S.; Lin, E.K.; Papareddy, R.K.; Xue, Y.; Jacobsen, S.E. Single-nucleus RNA-seq reveals that MBD5, MBD6, and SILENZIO maintain silencing in the vegetative cell of developing pollen. *Cell Rep.* **2022**, *41*, 111699. [[CrossRef](#)] [[PubMed](#)]
28. Misra, C.S.; Santos, M.R.; Rafael-Fernandes, M.; Martins, N.P.; Monteiro, M.; Becker, J.D. Transcriptomics of Arabidopsis sperm cells at single-cell resolution. *Plant Reprod.* **2019**, *32*, 29–38. [[CrossRef](#)]
29. Song, Q.X.; Ando, A.A.; Jiang, N.; Ikeda, Y.; Chen, Z.J. Single-cell RNA-seq analysis reveals ploidy-dependent and cell-specific transcriptome changes in Arabidopsis female gametophytes. *Genome Biol.* **2020**, *21*, 178. [[CrossRef](#)]
30. Kim, J.Y.; Symeonidi, E.; Pang, T.Y.; Denyer, T.; Weidauer, D.; Bezruczyk, M.; Miras, M.; Zöllner, N.; Hartwig, T.; Wudick, M.M.; et al. Distinct identities of leaf phloem cells revealed by single cell transcriptomics. *Plant Cell* **2021**, *33*, 511–530. [[CrossRef](#)]
31. Lopez-Anido, C.B.; Vatén, A.; Smoot, N.K.; Sharma, N.; Guo, V.; Gong, Y.; Gil, M.X.A.; Weimer, A.K.; Bergmann, D.C. Single-Cell Resolution of Lineage Trajectories in the Arabidopsis Stomatal Lineage and Developing Leaf. *Dev. Cell* **2021**, *56*, 1043–1055. [[CrossRef](#)]
32. Xu, X.; Crow, M.; Rice, B.R.; Li, F.; Harris, B.; Liu, L.; Demesa-Arevalo, E.; Lu, Z.; Wang, L.; Fox, N.; et al. Single-cell RNA sequencing of developing maize ears facilitates functional analysis and trait candidate gene discovery. *Dev. Cell* **2021**, *56*, 557–568. [[CrossRef](#)]
33. Omary, M.; Gil-Yarom, N.; Yahav, C.; Steiner, E.; Hendelman, A.; Efroni, I. A conserved superlocus regulates above- and belowground root initiation. *Science* **2022**, *375*, 993. [[CrossRef](#)]
34. Sun, X.; Feng, D.; Liu, M.; Qin, R.; Li, Y.; Lu, Y.; Zhang, X.; Wang, Y.; Shen, S.; Ma, W.; et al. Single-cell transcriptome reveals dominant subgenome expression and transcriptional response to heat stress in Chinese cabbage. *Genome Biol.* **2022**, *23*, 262. [[CrossRef](#)] [[PubMed](#)]
35. Conde, D.; Triozzi, P.M.; Pereira, W.J.; Schmidt, H.W.; Balmant, K.M.; Knaack, S.A.; Redondo-López, A.; Roy, S.; Dervinis, C.; Kirst, M. Single-nuclei transcriptome analysis of the shoot apex vascular system differentiation in Populus. *Development* **2022**, *149*, 200632. [[CrossRef](#)] [[PubMed](#)]
36. Qiu, D.; Bai, S.; Ma, J.; Zhang, L.; Shao, F.; Zhang, K.; Yang, Y.; Sun, T.; Huang, J.; Zhou, Y.; et al. The genome of Populus alba × Populus tremula var. glandulosa clone 84K. *DNA Res.* **2019**, *26*, 423–431. [[CrossRef](#)]
37. Wang, H.; Zhao, P.; He, Y.; Su, Y.; Zhou, X.; Guo, H. Transcriptome and miRNAs Profiles Reveal Regulatory Network and Key Regulators of Secondary Xylem Formation in “84K” Poplar. *Int. J. Mol. Sci.* **2023**, *24*, 16438. [[CrossRef](#)]
38. Xia, Y.; Cao, Y.; Ren, Y.; Ling, A.; Du, K.; Li, Y.; Yang, J.; Kang, X. Effect of a suitable treatment period on the genetic transformation efficiency of the plant leaf disc method. *Plant Methods* **2023**, *19*, 15. [[CrossRef](#)]
39. Wen, S.; Ge, X.; Wang, R.; Yang, H.; Bai, Y.; Guo, Y.; Zhang, J.; Lu, M.; Zhao, S.; Wang, L. An Efficient Agrobacterium-Mediated Transformation Method for Hybrid Poplar 84K (*Populus alba* × *P. glandulosa*) Using Calli as Explants. *Int. J. Mol. Sci.* **2022**, *23*, 2216. [[CrossRef](#)]
40. Murashige, T.; Skoog, F. A Revised Medium for Rapid Growth and Bio Assays with Tohaoco Tissue Cultures. *Physiol. Plant.* **1962**, *15*, 473–497. [[CrossRef](#)]
41. Du, K.; Liao, T.; Ren, Y.; Geng, X.; Kang, X. Molecular Mechanism of Vegetative Growth Advantage in Allotriploid Populus. *Int. J. Mol. Sci.* **2020**, *21*, 441. [[CrossRef](#)]
42. Zhu, X.; Zhang, Y.; Du, Z.; Chen, X.; Zhou, X.; Kong, X.; Sun, W.; Chen, Z.; Chen, C.; Chen, M. Tender leaf and fully-expanded leaf exhibited distinct cuticle structure and wax lipid composition in Camellia sinensis cv Fuyun 6. *Sci. Rep.* **2018**, *8*, 14944. [[CrossRef](#)]
43. Zheng, G.X.Y.; Lau, B.T.; Schnall-Levin, M.; Jarosz, M.; Bell, J.M.; Hindson, C.M.; Kyriazopoulou-Panagiotopoulou, S.; Masquelier, D.A.; Merrill, L.; Terry, J.M.; et al. Haplotyping germline and cancer genomes with high-throughput linked-read sequencing. *Nat. Biotechnol.* **2016**, *34*, 303–311. [[CrossRef](#)]
44. Butler, A.; Hoffman, P.; Smibert, P.; Papalexi, E.; Satija, R. Integrating single-cell transcriptomic data across different conditions, technologies, and species. *Nat. Biotechnol.* **2018**, *36*, 411–420. [[CrossRef](#)]
45. McGinnis, C.S.; Murrow, L.M.; Gartner, Z.J. DoubletFinder: Doublet Detection in Single-Cell RNA Sequencing Data Using Artificial Nearest Neighbors. *Cell Syst.* **2019**, *8*, 329–337. [[CrossRef](#)] [[PubMed](#)]
46. Macosko, E.Z.; Basu, A.; Satija, R.; Nemeshegyi, J.; Shekhar, K.; Goldman, M.; Tirosh, I.; Bialas, A.R.; Kamitaki, N.; Martersteck, E.M.; et al. Highly parallel genome-wide expression profiling of individual cells using nanoliter droplets. *Cell* **2015**, *161*, 1202–1214. [[CrossRef](#)] [[PubMed](#)]
47. Becht, E.; McInnes, L.; Healy, J.; Dutertre, C.; Kwok, I.W.H.; Ng, L.G.; Ginhoux, F.; Newell, E.W. Dimensionality reduction for visualizing single-cell data using UMAP. *Nat. Biotechnol.* **2018**, *37*, 38–44. [[CrossRef](#)] [[PubMed](#)]
48. Cao, Y.; Wang, X.; Peng, G. SCSA: A Cell Type Annotation Tool for Single-Cell RNA-seq Data. *Front. Genet.* **2020**, *11*, 490. [[CrossRef](#)] [[PubMed](#)]
49. Jin, J.; Lu, P.; Xu, Y.; Tao, J.; Li, Z.; Wang, S.; Yu, S.; Wang, C.; Xie, X.; Gao, J.; et al. PCMDB: A curated and comprehensive resource of plant cell markers. *Nucleic Acids Res.* **2022**, *50*, D1448–D1455. [[CrossRef](#)] [[PubMed](#)]

50. Qiu, X.; Hill, A.; Packer, J.; Lin, D.; Ma, Y.A.; Trapnell, C. Single-cell mRNA quantification and differential analysis with Census. *Nat. Methods* **2017**, *14*, 309–315. [[CrossRef](#)] [[PubMed](#)]
51. Neumann, M.; Xu, X.; Smaczniak, C.; Schumacher, J.; Yan, W.; Bluthgen, N.; Greb, T.; Jonsson, H.; Traas, J.; Kaufmann, K.; et al. A 3D gene expression atlas of the floral meristem based on spatial reconstruction of single nucleus RNA sequencing data. *Nat. Commun.* **2022**, *13*, 2838. [[CrossRef](#)]
52. Satija, R.; Farrell, J.A.; Gennert, D.; Schier, A.F.; Regev, A. Spatial reconstruction of single-cell gene expression data. *Nat. Biotechnol.* **2015**, *33*, 495–502. [[CrossRef](#)]
53. Skalak, J.; Vercruyssen, L.; Claeys, H.; Hradilova, J.; Cerny, M.; Novak, O.; Plackova, L.; Saiz-Fernandez, I.; Skalakova, P.; Coppens, F.; et al. Multifaceted activity of cytokinin in leaf development shapes its size and structure in Arabidopsis. *Plant J.* **2019**, *97*, 805–824. [[CrossRef](#)] [[PubMed](#)]
54. Javelle, M.; Vernoud, V.; Rogowsky, P.M.; Ingram, G.C. Epidermis: The formation and functions of a fundamental plant tissue. *New Phytol.* **2011**, *189*, 17–39. [[CrossRef](#)] [[PubMed](#)]
55. Zuch, D.T.; Doyle, S.M.; Majda, M.; Smith, R.S.; Robert, S.; Torii, K.U.; Sveriges, L. Cell biology of the leaf epidermis: Fate specification, morphogenesis, and coordination. *Plant Cell* **2022**, *34*, 209–227. [[CrossRef](#)] [[PubMed](#)]
56. Ho, C.K.; Bringmann, M.; Oshima, Y.; Mitsuda, N.; Bergmann, D.C. Transcriptional profiling reveals signatures of latent developmental potential in Arabidopsis stomatal lineage ground cells. *Proc. Natl. Acad. Sci. USA* **2021**, *118*, e2021682118. [[CrossRef](#)] [[PubMed](#)]
57. Pillitteri, L.J.; Torii, K.U. Mechanisms of Stomatal Development. *Annu. Rev. Plant Biol.* **2012**, *63*, 591–614. [[CrossRef](#)] [[PubMed](#)]
58. Flutsch, S.; Wang, Y.; Takemiya, A.; Violet-Chabrand, S.; Klejchova, M.; Nigro, A.; Hills, A.; Lawson, T.; Blatt, M.R.; Santelia, D. Guard Cell Starch Degradation Yields Glucose for Rapid Stomatal Opening in Arabidopsis. *Plant Cell* **2020**, *32*, 2325–2344. [[CrossRef](#)] [[PubMed](#)]
59. Vercruyssen, J.; Baekelandt, A.; Gonzalez, N.; Inzé, D. Molecular networks regulating cell division during Arabidopsis leaf growth. *J. Exp. Bot.* **2020**, *71*, 2365–2378. [[CrossRef](#)]
60. Wang, H.; Kong, F.; Zhou, C. From genes to networks: The genetic control of leaf development. *J. Integr. Plant Biol.* **2021**, *63*, 1181–1196. [[CrossRef](#)]
61. Boron, A.K.; Van Loock, B.; Suslov, D.; Markakis, M.N.; Verbelen, J.; Vissenberg, K. Over-expression of AtEXLA2 alters etiolated arabidopsis hypocotyl growth. *Ann. Bot.* **2015**, *115*, 67–80. [[CrossRef](#)]
62. Cosgrove, D.J. Plant expansins: Diversity and interactions with plant cell walls. *Curr. Opin. Plant Biol.* **2015**, *25*, 162–172. [[CrossRef](#)]
63. Schröder, F.; Lisso, J.; Lange, P.; Müssig, C. The extracellular EXO protein mediates cell expansion in Arabidopsis leaves. *BMC Plant Biol.* **2009**, *9*, 20. [[CrossRef](#)] [[PubMed](#)]
64. Du, K.; Jiang, S.; Chen, H.; Xia, Y.; Guo, R.; Ling, A.; Liao, T.; Wu, W.; Kang, X. Spatiotemporal miRNA and transcriptomic network dynamically regulate the developmental and senescence processes of poplar leaves. *Hortic. Res.* **2023**, *10*, uhad186. [[CrossRef](#)] [[PubMed](#)]
65. Allahverdiyeva, Y.; Suorsa, M.; Rossi, F.; Pavesi, A.; Kater, M.M.; Antonacci, A.; Tadini, L.; Pribil, M.; Schneider, A.; Wanner, G.; et al. Arabidopsis plants lacking PsbQ and PsbR subunits of the oxygen-evolving complex show altered PSII super-complex organization and short-term adaptive mechanisms. *Plant J. Cell Mol. Biol.* **2013**, *75*, 671–684. [[CrossRef](#)] [[PubMed](#)]
66. Mazor, Y.; Borovikova, A.; Caspy, I.; Nelson, N. Structure of the plant photosystem I supercomplex at 2.6 Å resolution. *Nat. Plants* **2017**, *3*, 17014. [[CrossRef](#)]

Disclaimer/Publisher's Note: The statements, opinions and data contained in all publications are solely those of the individual author(s) and contributor(s) and not of MDPI and/or the editor(s). MDPI and/or the editor(s) disclaim responsibility for any injury to people or property resulting from any ideas, methods, instructions or products referred to in the content.